LIGHTING DESIGN CONSIDERATIONS AND CHANNEL MODELING FOR VISIBLE LIGHT COMMUNICATIONS

A Thesis

by

Sadi Safaraliev

Submitted to the

Graduate School of Sciences and Engineering
In Partial Fulfillment of the Requirements for
the Degree of

Master of Science

in the
Department of Electrical and Electronics Engineering

Özyeğin University
June 2019

LIGHTING DESIGN CONSIDERATIONS AND CHANNEL MODELING FOR VISIBLE LIGHT COMMUNICATIONS

Approved by:

Professor Murat Uysal, Advisor,
Department of Electrical and
Electronics Engineering
Özyeğin University

Assistant Professor Ahmet Tekin,
Department of Electrical and
Electronics Engineering
Özyeğin University

Assistant Professor Tuncer Baykas,
Department of Electrical and
Electronics Engineering
Medipol University

Date Approved: 10 June 2019

To my family for their love, support and encouragement.

ABSTRACT

There has been an extensive work on visible light communication (VLC) mainly due to scarcity in radio frequency (RF) spectrum and urgent need for a new wireless communication system in the near future. VLC considers the dual use of LED luminaires as the light sources for illumination as well as signal sources for wireless communication applications. However, to the best of our knowledge, the existing works mainly overlook lighting design considerations which might have significant effects on the performance of VLC systems. In addition, there is a lack of proper VLC channel models which take into account wiring and cabling topologies.

In the first part of this thesis, we discuss some main indoor lighting design considerations and their implications for VLC applications. In particular, we consider some practical cabling topologies of LED luminaires and wiring topologies of LED chips within the luminaires. Based on non-sequential ray tracing, we obtain channel impulse responses (CIRs) and quantify the impact of cabling and wiring delays.

In the second part of thesis, we consider outdoor applications of VLC. We first discuss outdoor lighting design considerations and their possible implications on VLC system design. Based on ray-tracing approach, we obtain CIRs for an infrastructure-to-pedestrian (I2P) outdoor VLC scenario. Using these CIRs, we calculate channel DC gain, path loss, root mean square (RMS) delay spread and mean excess delay values.

ÖZET

Radyo frekansı (RF) spektrumundaki kıtlık ve yakın gelecekte yeni bir kablosuz haberleşme sistemine acil ihtiyaç nedeniyle görünür ışık haberleşmesi (visible light communication – VLC) üzerine kapsamlı bir çalışma yapılmıştır. VLC, LED aydınlatma armatürlerinin hem aydınlatma için ışık kaynağı hem de kablosuz haberleşme uygulamaları için sinyal kaynağı olarak kullanımını ele alır. Bununla birlikte, bildiğimiz kadarıyla, mevcut işler çoğunlukla VLC sistemlerinin performansı üzerinde önemli etkileri olabilecek aydınlatma tasarımına dikkat etmemektedir. Ek olarak, hem LED armatürlerinin hem de armatürlerdeki LED'lerin kablolama topolojilerini dikkate alan uygun VLC kanal modelleri eksikliği vardır.

Bu tezin ilk bölümünde bazı ana iç mekan aydınlatma tasarımı hususlarını ve bunların VLC uygulamaları üzerindeki etkilerini tartışıyoruz. Özellikle, LED armatürlerde bazı pratik kablolama topolojilerini ve armatürlerdeki LED yongalarının kablolama topolojilerini dikkate alıyoruz. Sıralı olmayan ışın izlemeye dayanarak, kanal dürtü yanıtlarını (channel impulse responses – CIR'lar) elde edip LED ve armatür kablolama gecikmelerinin etkisini ölçüyoruz.

Tezin ikinci bölümünde, VLC'nin dış mekan uygulamalarını ele alıyoruz. Öncelikle dış mekan aydınlatma tasarımını ve bunların VLC sistem tasarımı üzerindeki olası sonuçlarını tartışıyoruz. Işın izleme yaklaşımına dayanarak, altyapıdan yayaya (infrustructure-to-pedestrian – I2P) dış mekan VLC senaryosu için CIR'ları elde ediyoruz. Bu CIR'ları kullanarak, kanal DC kazancı, yol kaybı, kök ortalama kare (RMS) gecikme yayılımını ve ortalama aşırı gecikme değerlerini hesaplıyoruz.

ACKNOWLEDGMENTS

Throughout the writing of this thesis I have received a great deal of support and assistance. I would first like to thank my supervisor, Prof. Murat Uysal, whose patient guidance, expertise and constructive suggestions were invaluable during the planning and development of this research work. His prompt responses to my questions and queries and willingness to give his time so generously has been very much appreciated. I would also like to offer my special thanks to Dr. Farshad Miramirkhani for the assistance he has provided during my thesis work.

I am particularly grateful to the members of my thesis committee, Dr. Ahmet Tekin and Dr. Tuncer Baykas for carefully reviewing my thesis and for their time serving in my committee.

I wish to acknowledge my current company Vestel Electronics Corp. for offering me their resources in collection of my data. I would also like to express my very great appreciation to my colleagues at Vestel for their support, especially to Dr. Kadir Vahaplar and Emine Burcu Damar for their assistance with the street lighting standards.

Heartfelt thanks go to Madina, my wife, for her continuous help and support, without which I would not have come this far.

My special thanks are extended to my brother, Mehrubon Safaraliev, for his guidance and suggestions in my educational and professional journey and also for his emotional and financial support.

Last, but not least, I would like to express my very great appreciation to my parents for their unconditional support and encouragement not only during my study, but throughout my life.

TABLE OF CONTENTS

LIST OF TABLES

LIST OF FIGURES

CHAPTER I

INTRODUCTION

1.1 Motivation

Today, wireless communication technologies heavily rely on radio frequency (RF) bands of the electromagnetic spectrum. However, there are some serious drawbacks of RF spectrum. The main shortcoming of RF-based wireless communication technologies is the scarcity in RF spectrum. A recent market analysis report [1] shows that the global mobile data traffic grew 63% in 2016 and the monthly global mobile data traffic will reach 49 exabytes by 2021, which was 4.4 exabytes per month at the end of 2015 and 7.2 exabytes per month at the end of 2016. The total RF data traffic exceeded 11 exabytes per month in 2017, creating a 97% gap between available capacity of mobile networks and the data traffic demand per device [2]. The increasing data consumption per mobile device, like data-intensive mobile multimedia and cloud-based applications, is one of the main reasons for this huge amount of data traffic [3]. Another reason is the explosively growing number of connected devices as a result of development of new technologies like the Internet of Things (IoT). A research [4] predicts the number of connected devices to reach 100 billion by 2025. On the other hand, the RF spectrum is a small licensed part of electromagnetic spectrum which is nearly fully being used with heavy regulations and will not be able to cope with increasing data traffic. This scarcity in RF spectrum makes it difficult to improve the capacity of wireless networks and to initiate new wireless services for mobile network operators [5].

Another main problem is the vulnerability of wireless transmissions to RF interference from various sources [6] which is the main reason for heavy regulations on and licensing of RF spectrum for use in wireless access technologies. This is a growing problem for technologies that use unlicensed frequency bands to operate, since the use of these bands is increasing over time [7]. Interference happens when waves/signals of similar frequencies superpose, giving result to adding up of the waves/signals when they are in-phase (i.e., constructive interference) or canceling out when they are out-of-phase (i.e., destructive interference) [8]. Interference of signals with waves generated by other sources creates disturbance on the signals where the signals will be completely lost when they undergo destructive interference. For example, the signals produced by electronic devices like smartphones can interfere with emergency signals of the airplane. This is the reason why our smartphones have an "airplane mode" in order to prevent such possible interferences that, otherwise, may cause catastrophic results. Another example of interference is jamming, which is the intentional generation of interference for denial-of-service attack [9]. In other words, RF signals can easily be blocked using jammers.

Another drawback of RF transmissions is their prohibition in some areas due to safety and security reasons. These technologies are not allowed to be used for control applications and safety-related instrumentation in some areas like power plants, nuclear plants, petrochemical industry and hospitals. This prohibition is due to sensitivity of equipment used in these areas to electromagnetic radiations [10], cyber security problems due to transparency of walls to RF signals which makes the transmitted data accessible to cyber-attackers outside of these areas [11] and so on [12]. However, these places need fast and inter-connected data systems for proper monitoring and efficient operation. The

savings that a proper monitoring at a single power plant provides can reach hundreds of thousands of dollars [13].

In the consideration of the above issues and drawbacks, the demand for a new ubiquitous broadband wireless access technology is increasing. Different solutions are currently being discussed and proposed to meet the requirements of future wireless networks [14]. One of these solutions is to utilize optical spectrum for wireless communication purposes. Throughout history, humanity has developed different optical signaling methods and techniques for wireless communication purposes. Using smoke or fire for sending messages dates back to ancient times. Polished plates made up of metallic materials were used by Romans to send messages to long distances by reflecting the sunlight. In the 1790s, a primitive version of optical communication, semaphore lines systems were developed [15]. In the early 1800s, so-called heliograph was developed based on the use of a mirror to reflect flashes of sunlight based on Morse code, where the flashes were obtained by either momentarily pivoting the mirror or using a shutter to interrupt the beam [16]. In 1880, A. Graham Bell invented the photophone [17] and was able to transmit a voice signal over a transmission range of more than 200 meters. In this device, the reflected sunlight by a flexible mirror is vibrated by the projection of the sound on the mirror and these vibrations are converted into electrical signals by a selenium cell at the receiver side using selenium's photoconductive properties [18]. The electrical signals are, then, converted back into sound waves by an amplifier or speaker.

The photophone never came out as a commercial product due the fact that there is no known way to control the sunlight as an efficient light source. However, recent advancements in light emitting diodes (LEDs) pave the way for visible light communication (VLC) [19], also known as LiFi, where LEDs are deployed as wireless

transmitters. It deploys the unlicensed visible light spectrum that ranges roughly from 380 nm (789 THz) to 780 nm (384 THz). VLC involves the dual use of LEDs for communication purposes by modulating the LEDs at very high speeds that are not noticeable to human eye while being used as illumination sources. It is also meant to be a bidirectional and multiple-input multiple-output network [20]. Having a large bandwidth capacity, being immune to electromagnetic interferences and offering a secure wireless communication due to opacity of walls to visible light, VLC offers a complete solution for future short-range wireless networks. Therefore, VLC is considered as a complementary wireless access technology to WiFi or cellular networks.

The first demonstrations of VLC started in early 1990's and the first implementation took place in 2003 [21]. Using white LED luminaires for indoor communication applications was first proposed in 2004 [22]. With emergence and development of inexpensive LEDs VLC systems have improved, offering research and applications in various areas like position detection, intelligent systems, image sensor communication, audio applications, networking and aesthetics [23]. The practical functionality of VLC was demonstrated in July 2011 [24]. VLC systems have been implemented in various places, like in a museum displaying a multimedia content in order to improve the visual experience of each artwork and guide the visitors in the museum according to their wishes or interest [25]. An indoor positioning system (IPS) based on VLC technology was installed in a hypermarket on May 2015 which allowed its customers to locate the products promotion where the location accuracy of this VLC system was less than 1 meter [26]. Another IPS project was introduced in 2016 [27] which used LED luminaires for broadcasting positioning signals via amplitude modulation of light without surpassing lighting requirements and it has already been adopted by some

leading LED lighting companies [28, 29]. LiFi battens that could offer data speeds of up to 43 Mb/s and a LED downlight that embedded all necessary LiFi components while supporting up to 16 users at the same time with data speeds of 45 Mb/s were introduced in an exhibition in November 2017 [30]. The first LiFi panel light was introduced in an exhibition in January 2018, which was capable of a download speed of 108 Mb/s and an upload speed of 53 Mb/s with a coverage of 48 square meters [31]. With future advancements, VLC technology would offer outstanding applications in variety of fields such as aviation [32], big data and IoT. See [33, 34] for an extensive survey on VLC.

1.2 Fundamentals of VLC Systems

The data in a VLC system is transmitted by modulating the light intensity of LEDs with high frequencies, far beyond the frequencies that a human being can notice. In other words, the data signals in a VLC system are variations in light intensity of light sources with high frequencies.

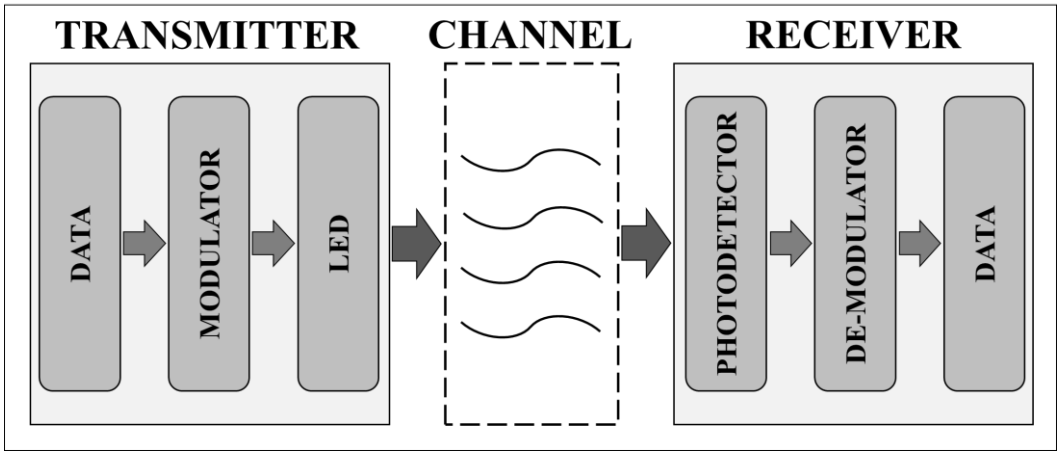

Figure 1: Schematic representation of a VLC system

As illustrated in Figure 1, a VLC system is mainly composed of a transmitter module, a channel and a receiver module. The transmitter module in a VLC system

includes the data source, the modulator and the LED. The modulator converts the source data into electrical current signals which are added to the DC current used for driving the LED. Instead of modulating the data into voltage signals, it is better to modulate the data in a VLC transmitter into current signals due to electro-optical characteristics of LEDs. The LED, then, emits a light with modulated overall intensity, where the modulations in light intensity are almost linearly proportional to the modulated driving DC current. A type of modulated light output that is used for both illumination and VLC is schematically illustrated in Figure 2. For such a modulated light output we would perceive a constant light intensity around 100% which is the average of the overall intensity. When we use multi-color LEDs in the transmitter, each color would be considered as a different antenna.

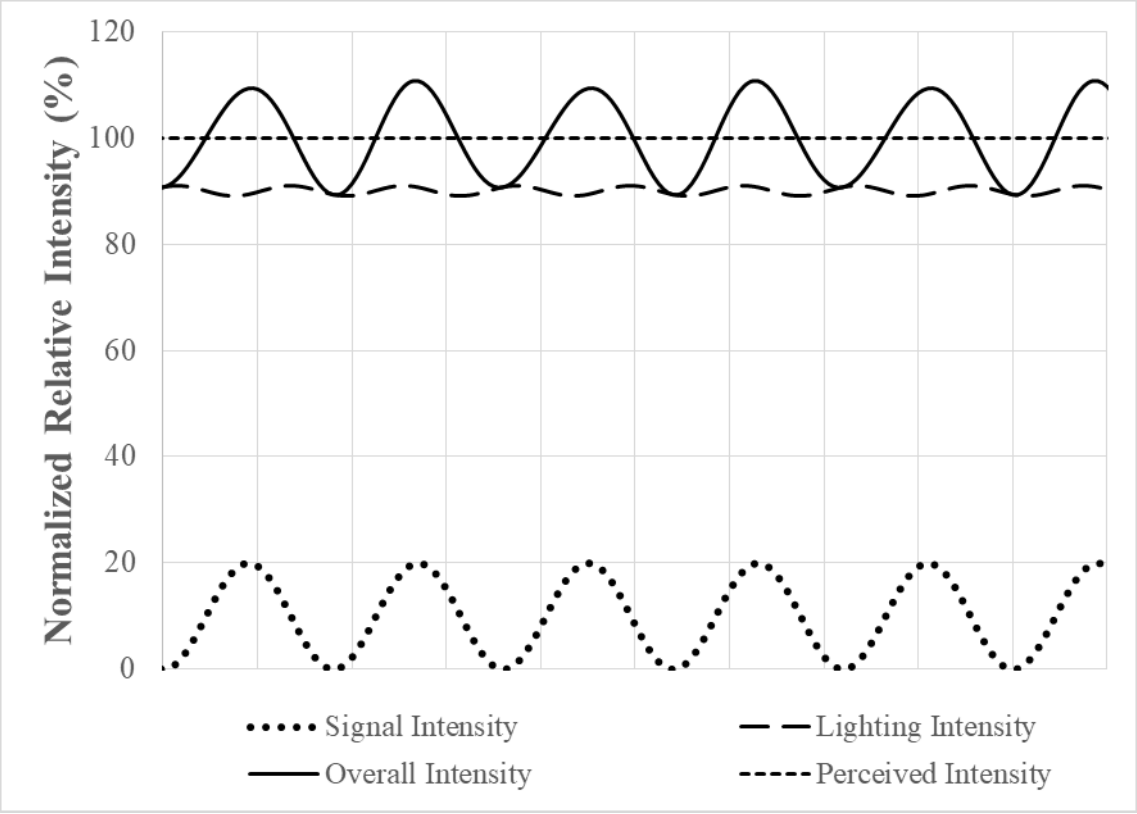

Figure 2: Schematic representation of a modulated light intensity that is used for both illumination and VLC

The transmitted signal goes through the channel. The receiver of a VLC system is a module that detects and de-modulates the carrier signal to obtain the transmitted data. The signal, including the noise, is detected by the photodetector (PD), either a photodiode or a phototransistor, which converts it into electrical voltage signal and sends it to demodulator. The demodulator, then, demodulates this signal to obtain the transmitted data.

1.3 Motivation of Thesis

Recently, there has been an extensive work on VLC channel modeling including both fixed [35, 36, 37, 38, 39, 40] and mobile [41, 42, 43] scenarios. These works discuss several indoor scenarios and lighting conditions. However, existing works mainly overlook the luminaire characteristics. A LED luminaire typically consists of multiple LED chips. Wiring topology refers to how LED chips are connected within the luminaire. In a typical indoor environment, there exist multiple luminaires. Cabling topology refers to how the luminaires are connected to the communication access point. However, to the best of our knowledge, there is only one previous work that discusses the effect of cabling and wiring topologies [44]. In [44], Ren *et al.* introduce a recursive channel model based on Barry's method [40] taking into account wiring and cabling delays. The work in [44] is limited to the assumptions of only purely diffuse reflections and ideal Lambertian source which might not hold true for many practical cases. Moreover, as far as we know, there is no previous work that provides a discussion of lighting design considerations for indoor VLC.

VLC can be considered for outdoor applications as well. Currently, most of the researches and applications are mainly focused on indoor VLC with less attention to

outdoor VLC due to problems like lower received power and lower SNR. Nevertheless, a huge amount of achievements have already been reported on outdoor VLC [45, 46]. However, to the extent of our knowledge, there is no previous work that discusses the impact of lighting design parameters on outdoor VLC systems. Our work shows that received optical signal power and consecutively SNR can be improved by optimizing some outdoor lighting design parameters such as luminaire design and luminaire installation parameters. Furthermore, the existing works on outdoor VLC are mainly focused on vehicular (V2V, V2I/I2V [46]), building-to-building (B2B) and considering park and street lights as access points [45]. On the other hand, there are various possible compelling outdoor infrastructure-to-pedestrian (I2P) VLC applications like outdoor positioning systems. However, we believe that our work is the first to consider an I2P outdoor VLC channel modeling with a realistic ray tracing approach.

The objective of our work is mainly to develop realistic VLC channel models for indoor and outdoor environments in addition to comprehensive analyses of the effects of some essential lighting design parameters on VLC channels. Our study is based on non-sequential ray tracing features of Zemax® [47], a commercial optical and illumination design software [48], which is able to accurately describe the light interactions within a specified environment.

The first part of our work focuses on indoor lighting design considerations and channel modeling. We provide a thorough analysis of some crucial LED lighting design parameters and their possible effects on VLC systems. Next we adopt a realistic indoor channel modeling approach [39] to obtain CIRs and corresponding channel frequency responses.

In the second part of our work, we focus on the outdoor applications. First, we discuss the outdoor lighting design considerations and present a street lighting luminaire installation design following relevant illumination standards. Second, we model the channel between street lighting luminaires and a pedestrian. The luminaires are considered as transmitter antennas while the mobile phone of the pedestrian is used as a receiver. The asymmetrical illumination patterns of the street lights is carefully taken into account. For the scenario under consideration, we obtain CIR and calculate channel DC gain, path loss, root mean square (RMS) delay spread and mean excess delay.

Some of the main ideas of this thesis have already been published by the author during his research. The results on the effect of wiring and cabling topologies on VLC can be found in [49] and [50].

1.4 Organization

The rest of the thesis is organized as follows. In Chapter II, we provide a detailed discussion of indoor lighting considerations for VLC applications and adopt a realistic indoor VLC channel modeling approach [39] for different cabling and wiring topologies based on non-sequential ray tracing features of Zemax®. In Chapter III, we focus on outdoor VLC channel modeling. We carry out a thorough analysis of outdoor lighting design considerations for VLC systems and provide our outdoor channel modeling scenario between street lighting luminaires and a pedestrian. Finally, we summarize and conclude this thesis in Chapter IV.

CHAPTER II

INDOOR LIGHTING DESIGN CONSIDERATIONS AND CHANNEL MODELING

2.1 Introduction

The existing works on indoor VLC mainly overlook the characteristics of lighting infrastructure and luminaire design that might have implications for VLC system design. A luminaire typically consists of multiple LED chips. Wiring topology refers to how LED chips are connected within the luminaire. In a typical indoor environment, there exist multiple luminaires. Cabling topology refers to how the luminaires are connected to the communication access point. Based on the type and length of cabling/wiring, significant delays can be introduced which should be taken into account in channel modeling.

In this chapter, we first consider some main indoor lighting design parameters and discuss their impacts on VLC, on indoor VLC in particular. Next, we adopt a ray tracing based VLC channel modeling approach [39] and present simulations for various cabling and wiring topologies. Then, we obtain CIRs for each topology and quantify the impact of wiring and cabling delays on CIRs.

2.2 Indoor Lighting Design Considerations

2.2.1 LEDs

LEDs are semiconductor devices which have a p-n junction made of at least two materials where the light of a particular color is produced depending on the materials used. The white light using LEDs is produced using different color mixing techniques

[51]. The most popular white LEDs are phosphorescent LEDs which have a blue light LED dye embedded in a layer of phosphor, commonly a yellow phosphor. In these LEDs, a portion of blue light passes the phosphor layer, a portion is converted into longer wavelengths, like green, yellow and red, by the phosphor and a small portion of blue light is lost. The combination of emitted colors is, then, seen as white light. The main disadvantage of using these LEDs for VLC applications is the longer decay lifetimes of converted light by the phosphorescence effect [52] which would decrease both the ON-OFF switching speed and bit rate. However, high bandwidths and/or the use of spectrally-efficient modulation schemes can provide high-speed communication [53]. For example, using a blue optical filter on the PD side would get rid of the converted portion of the white light, but it would decrease the signal power [54, 55, 56, 57, 58]. Another solution is improving white LEDs for VLC with shorter phosphor decay lifetimes. For instance, the colloidal quantum dot light-emitting devices (QD-LEDs) have shorter phosphorescence lifetimes, of the order of nanoseconds, which would enable faster switching rates for LEDs [59]. However, they have low efficacies (~65 lumens per watt) and long-term exposure to cadmium telluride (CdTe) quantum dots would cause functional impairments in live cells [60]. Therefore, they would not be preferred for use in general lighting applications. To give another example, a research [61] found out that a combination of perovskite nanocrystals and a red phosphor can support visible light communication modulation rates of 491 MHz with a capacity of transmitting a high data rate of up to 2 Gbps.

Another type of white light LEDs is a red-green-blue (RGB) LED where the white light is produced as a combination of red, green and blue colors. The red, green and blue colors can be modulated separately to obtain different colors or x-y chromaticity

coordinates on CIE 1931 color space [62, 63], as shown in Figure 3, with 2^3=8 different outputs, as illustrated in Figure 4. Deploying RGB LEDs for VLC applications can triple the data transmission. However, they would cause more complications both at the transmitter and the receiver sides with higher costs.

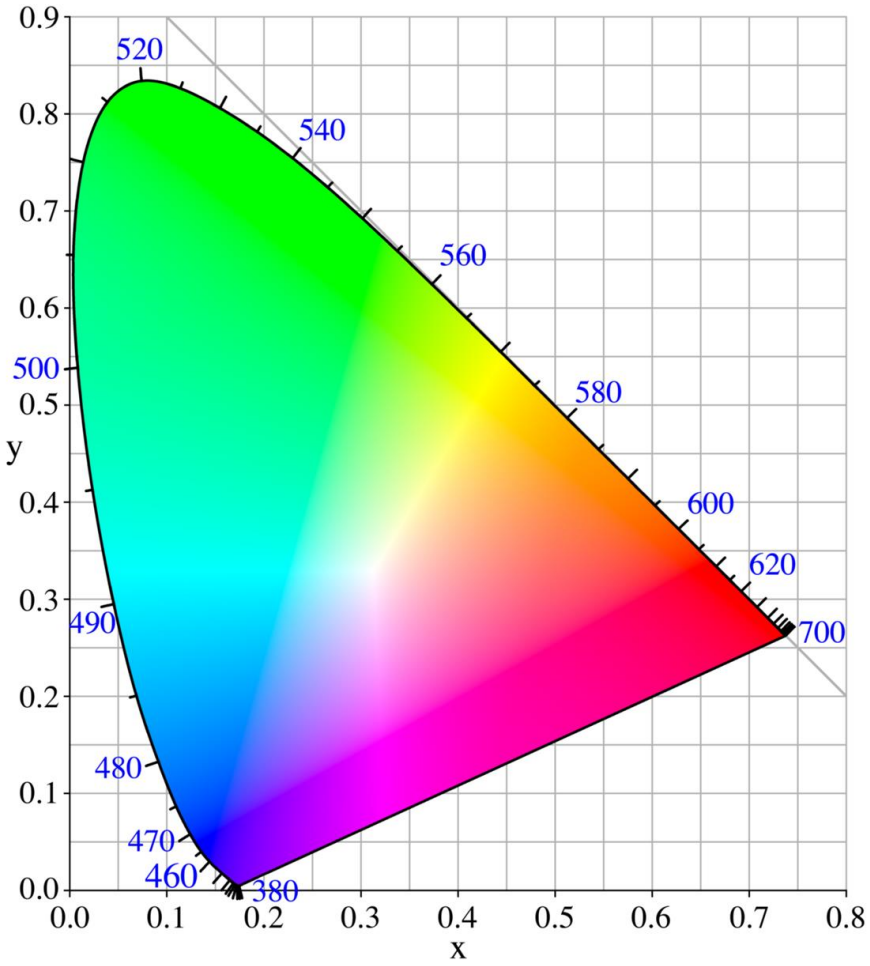

Figure 3: CIE 1931 x-y color space

In most of the current white LEDs, e.g., phosphorescent and RGB LEDs, there is a peak in blue spectrum which may cause disturbance in people's sleep patterns and harm nocturnal animals [64, 65, 66]. Low-intensity blue light exposure in the evening may also cause suppression of energy metabolism and drowsiness in the next morning [67]. The ideal light sources with minimal risks are the ones with closest properties to natural light

sources, especially to that of the sun. Some industrial LED companies have already produced LEDs that produce a white light with a spectral power distribution (SPD) that mimics the SPD of the sun [68, 69] which cause a decrease in eye fatigue and an improvement in sleeping quality [70]. However, these LEDs also produce white light via phosphorescence effect and phosphorescence has longer decay lifetimes than LED dyes that cause extra delays in CIRs than that of the LED dyes.

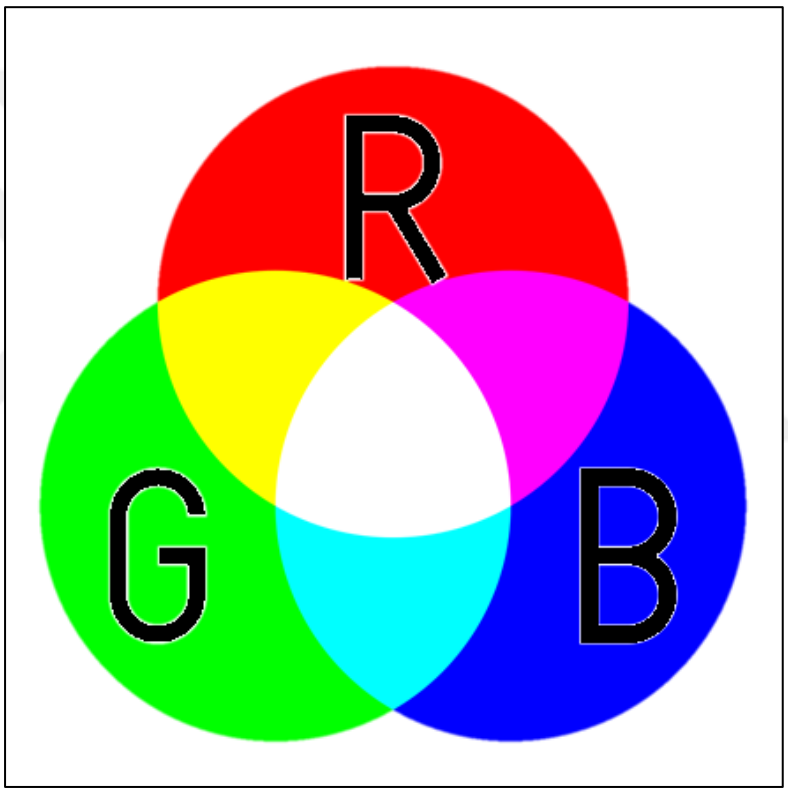

Figure 4: Color combinations of RGB

Each type of currently available LEDs have their advantages and disadvantages for lighting, communication or both applications. Hence, it is clear that either current LEDs need to be improved or new LEDs need to be developed and produced for dual-use in a VLC system for cost-effective and efficient illumination and high-speed communication applications.

2.2.2 Electro-optical Characteristics of LEDs

Electro-optical characteristics of LEDs play important roles for both illumination and communication applications. For a typical LED, forward voltage (V_f) and luminous flux (i.e., light output) would be within some ranges at a particular forward current (I_f). For example, a single LM281B+ CRI 80 LED, a Samsung middle power LED, would have a V_f between 2.8 V and 3.3 V while outputting a luminous flux between 52.5 lumens (lm) and 74 lm when driven at a typical I_f of 150 mA with solder temperature (T_s, using which junction temperature (T_j) can be calculated) of 25^0C [71]. These ranges are huge when considered for lighting applications. Therefore, LED manufacturers make binning of LEDs which is grouping the LEDs based on their optical and electrical properties. Samsung has separated LM281B+ CRI 80 LEDs into five voltage bins with 0.1 V separations and into four luminous flux bins with 4 lm separations [71]. These binnings are highly important for both lighting and VLC applications since they determine the electrical and optical tolerances of a luminaire.

The relationship between I_f and V_f of LEDs is exponential, i.e., I_f changes exponentially with changes in V_f. However, the luminous flux, which is directly proportional to luminous intensity (I_v), changes almost linearly with I_f. This means that luminous flux changes exponentially with V_f. Figure 5 shows relative luminous flux and V_f relationships with I_f of Samsung LM281B+ CRI 80 LED.

Electro-optical characteristics of LEDs show that it is better to drive LEDs of a luminaire with a constant current, instead of a constant voltage, to have a better control over light output of the luminaire with tighter tolerances. For further clarification,

consider two LM281B+ CRI 80 LEDs, LED1 and LED2, with a CCT of 4000K from A3 V_f bin (3.0-3.1 V) and SG luminous flux bin (70-74 lm) at the typical I_f of 150 mA and T_s of 25^0C. So, the V_f tolerance of these LEDs is about ±1.6% with luminous flux tolerance of about ±2.8%. Also assume that LED1 has 3.0 V and LED2 has 3.1 V where both have the same light output of 72 lm when driven with their typical I_f of 150 mA at T_s of 25^0C.

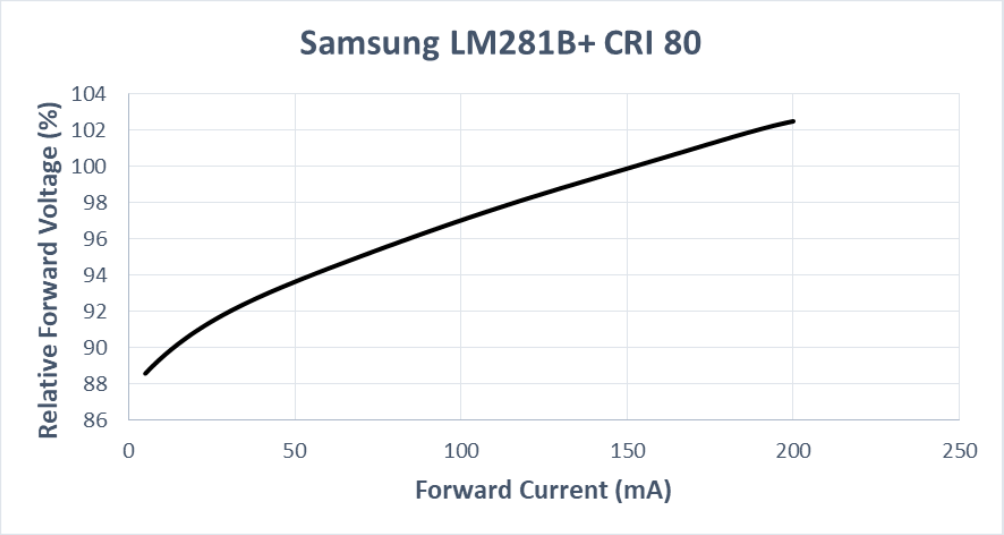

(a)

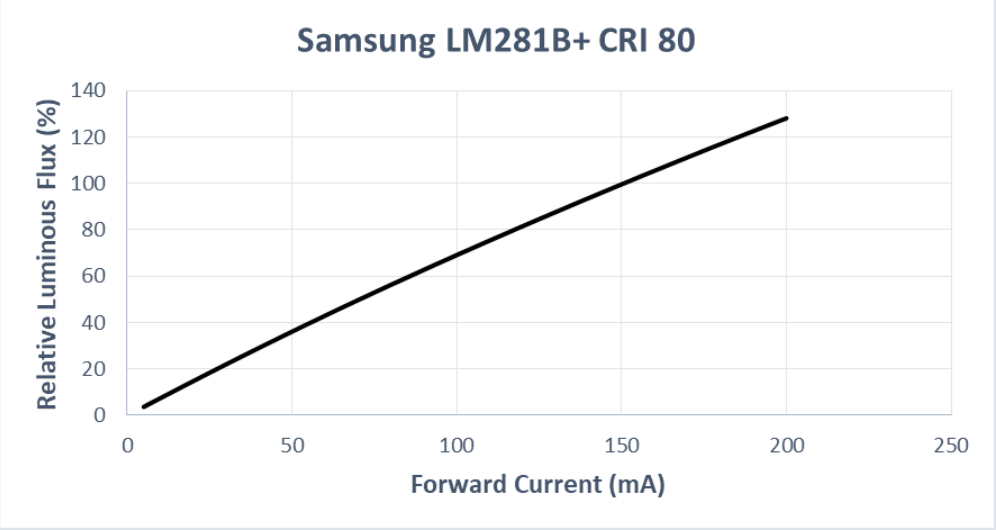

(b)

Figure 5: (a) electrical and (b) electro-optical characteristics of LM281B+ CRI 80

When these LEDs are driven with a constant V_f of 3.0 V, with a simple calculation from I_f and V_f graph data in Figure 5.a, we find out that when the voltage of LED2 is decreased from 3.1 V to 3.0 V (3.2% decrease), its I_f would be 95 mA (37% decrease). From Figure 5.b it can be calculated that when I_f of LED2 is decreased from 150 mA to 95 mA, its light output would decrease from 72 lm to 47.5 lm (34% decrease). Since LED1 and LED2 would give light outputs of 72 lm and 47.5 lm at 3.0 V, respectively, then there would be a decrease of 34% in light output of LED2 as compared to LED1 with only a 0.1 V or 3.2% decrease in V_f of LED2. This means that even if we use LEDs from single V_f and single luminous flux bins, it is possible that there was about 34% difference in light outputs of two LEDs when driven with a constant voltage. In other words, driving LEDs in a luminaire with a constant driving voltage would result in huge light output tolerances. Furthermore, these huge changes in light output with small changes in V_f would make it difficult to precisely generate and modulate optical data signals for VLC purposes, especially for modulations like in Figure 2. Therefore, it is better to drive the LEDs of a luminaire with constant driving currents both for illumination and VLC purposes.

It is important to make sure that all LEDs in a luminaire are driven with the same or similar I_f values. Consider a parallel wiring connection of abovementioned two LM281B+ CRI 80 LEDs (1S2P wiring connection), as schematically shown in Figure 6. Suppose that these LEDs are driven with a total constant current of I_{tot} in such a way that the voltage over both LEDs was 3.0V due to parallel connection. Then I_{tot} would be divided into two strings according to each LED's I_f and V_f relationships. As discussed above, there would be a differences of 37% in I_f and 34% in luminous flux of these LEDs.

This would result in inhomogeneous heat distribution and make the thermal management of the luminaire less efficient. In addition, different light outputs from different LEDs would result in non-uniform brightness of the light emitting area of the luminaire which is not preferred, especially for diffuse indoor lighting luminaires. Accordingly, it is important to drive all LEDs in a luminaire with the same or similar I_f values.

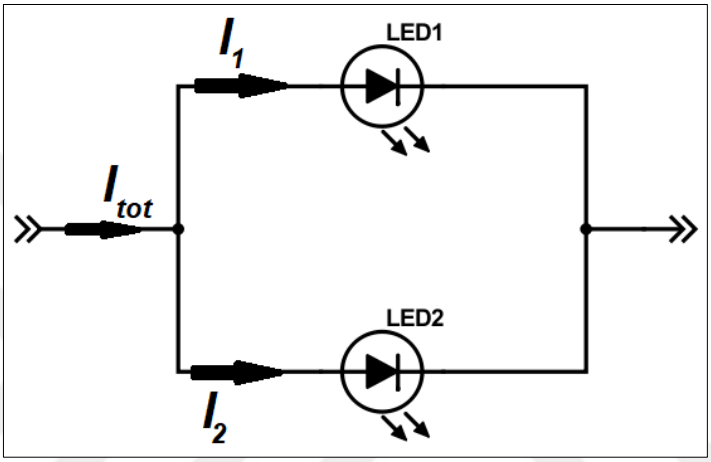

Figure 6: Schematic representation of two LEDs connected in parallel

2.2.3 Cabling Topologies

In a typical indoor environment, there exist multiple luminaires. In general, LED luminaires are designed to operate with available AC electric sources. Since the available AC sources have fixed voltages, e.g., 120 V, 220 V or 240 V, the LED luminaires are connected in parallel to have the same voltage over all luminaires. We assume that a data cable (CAT 5) runs in parallel to the electrical cable. It is also possible to use Power over Ethernet (PoE) to feed both data and power. We assume the deployment of a central access point (AP) where the LED luminaires (that act as transmitters) are connected. For connection, we consider two cabling topologies as illustrated in Figure 7. In the first topology (Figure 7.a), the data/electrical cables are terminated at the middle of luminaires.

The length of cable between the access point and each luminaire is the same. In the second topology (Figure 7.b), the length of cable for each luminaire changes. Difference in two topologies will not have any effect on illumination performance but the communication performance might be affected due to different cable lengths. For instance, when a signal is sent from AP to luminaires, all of the luminaires in Figure 7.a would receive it at the same time. On the other hand, in Figure 7.b, luminaire pairs (L_2 and L_3) and (L_1 and L_4) would receive it at the same time while there would be a particular delay between two pairs based on the cable length differences.

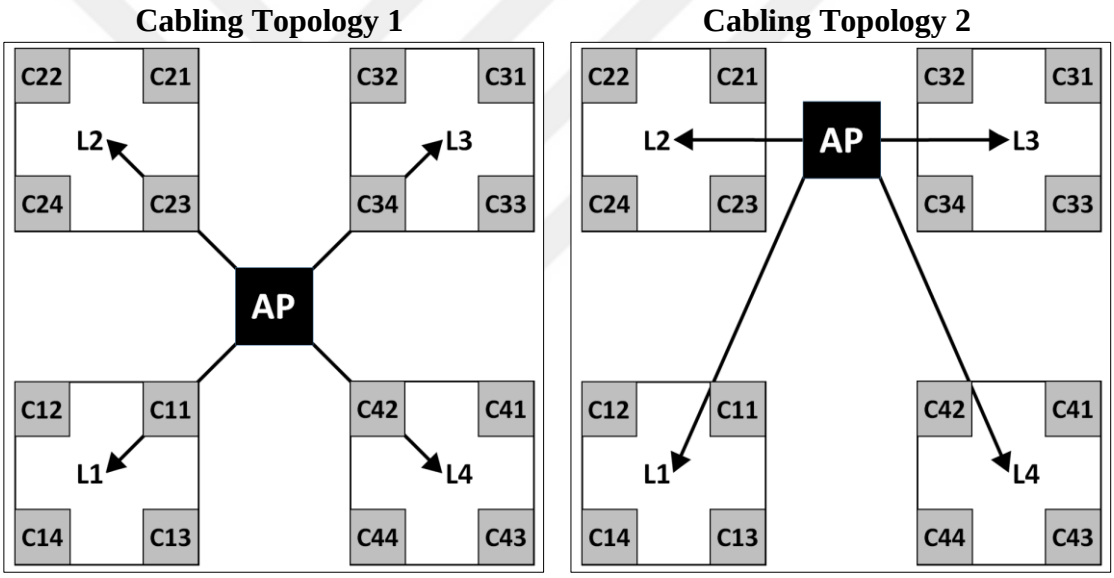

Figure 7: Cabling topologies under consideration

In a typical lighting application, especially when large numbers of luminaires are used, the cabling topology is designed to have minimum amount of total cabling length to minimize the cost. For instance, the cabling topology in Figure 7.b can be replaced with the cabling topology shown in Figure 8 to minimize the total cabling length (note that both topologies would have similar delaying effects). It is possible different signal delays between the luminaires due to unequal cabling lengths by using a separate cable

of equal length for each luminaire, even for the ones that are near the AP/electrical source. However, this would increase the amount of cables used, hence increase the cost.

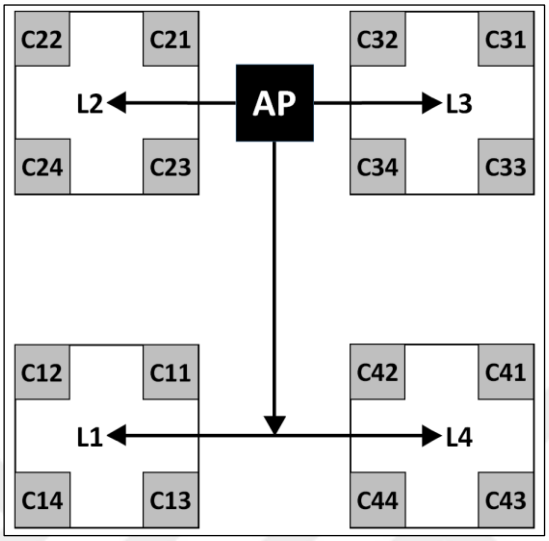

Figure 8: An actual cabling topology of 4 luminaires

2.2.4 Wiring Topologies

The wiring topology is more complicated than the cabling topology. In a LED luminaire, the LED chips can be connected in series, in parallel or some combination. The choice of wiring topology mainly depends on the number, type and characteristics of LED chips, their driving I_f and V_f as well as the output current and voltage of the power supply unit (PSU) in the LED luminaire. There are two types of PSUs, i.e., constant current PSUs and constant voltage PSUs. A constant current PSU has an output of fixed current with a variable voltage within a particular range. These PSUs vary the voltage with respect to load while keeping the current constant. On the other hand, a constant voltage PSU does the reverse, i.e., varies the current within a range while keeping the output voltage constant. In LED luminaires, because of the significant changes in I_f and relative luminous flux with small changes in V_f, constant current PSUs are typically

preferred to have more control over total light output of luminaires and uniformity of light output, as extensively discussed in section 2.2.2.

Connecting large numbers of LEDs in series would require PSUs with high DC output voltages, since the total driving voltage would be the sum of voltages over all LEDs. For instance, a luminaire with 100 LEDs connected in series with LED I_f of 150mA and V_f of 3V would require a PSU of DC output current of 150mA and output voltage around 300V. Considering that the available AC electrical sources are typically 240V or less, producing PSUs of higher voltages would be difficult and expensive since they need special components to handle high voltages. High voltages would also cause some reliability and safety issues like difficult isolation and touch problem. In addition, when a single LED is burned out, it would not allow any current flow, resulting in termination of current flow through all LEDs. Overcoming this would require using extra components like Zener diodes. On the other hand, connecting large numbers of LEDs in parallel would require PSUs with high DC output currents, since the total driving current would be the sum of currents over all LEDs. Producing such PSUs would also be difficult and expensive due to requirement for special components that could handle high current flows. Although burning out of an LED would not prevent the operation of other LEDs in a parallel wiring connection, all LEDs need to have exactly the same (or very close) V_f values to avoid current hogging and non-uniformity in brightness of LEDs. However, this is difficult to achieve since LEDs have some V_f tolerances and small changes in V_f can cause huge changes in I_f. Most of LED luminaires have tens or hundreds of LEDs. Therefore, LED luminaires with few LEDs typically have either fully parallel or fully series connections. On the other hand, in luminaires with large numbers of LEDs some combinations of parallel and series connections of LEDs are considered to minimize the

problems with both fully parallel and fully series wiring connections of large numbers of LEDs. To make sure that the current flow is the same over all parallel strings of LEDs, the use of some current balancing circuitry can be considered.

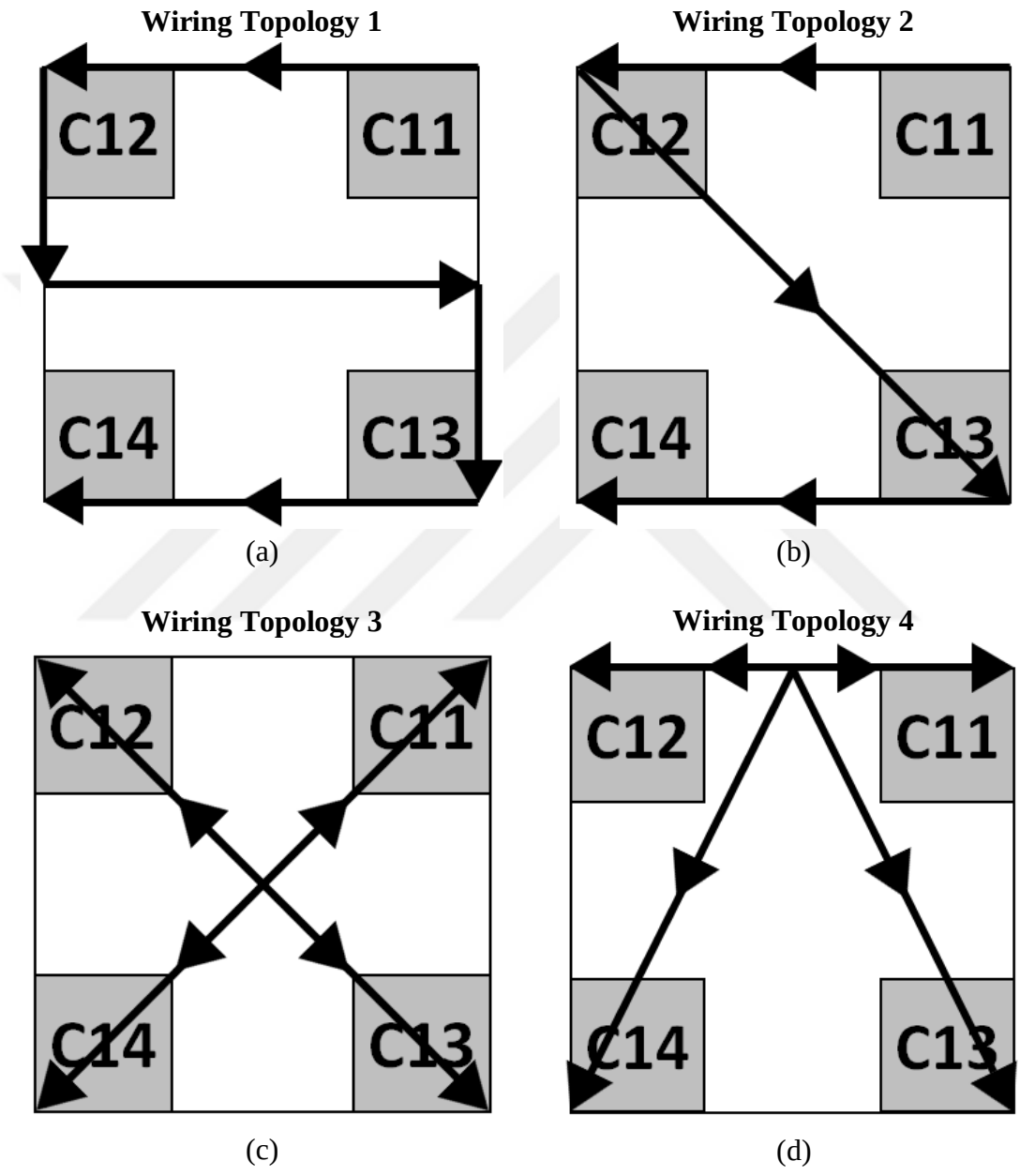

Figure 9: Wiring topologies under consideration

According to the above considerations, four different wiring topologies are presented in Figure 9. Without loss of generalization, only the luminaire L_1 (Figure 7) is

considered. In Figure 9.a and Figure 9.b, four LED chips $C_{1,i}, i = 1, \dots, 4$, are connected in series. In Figure 9.c and Figure 9.d, LED chips are connected in parallel. In Figure 9.a and Figure 9.b, all of the four LED chips would have the same I_f as desired for uniform illumination. In Figure 9.c and Figure 9.d, all of the four LED chips would have the same V_f values. This indicates that similar I_f values will flow through each LED chip if their V_f differences are sufficiently low. In the following section, we only consider fully series (Figure 9.a and Figure 9.b) and fully parallel (Figure 9.c and Figure 9.d) connections of four LEDs to highlight the differences.

2.3 Channel Modeling for Indoor VLC

For channel modeling, we use the ray tracing and channel modeling approach described in [39]. We take advantage of non-sequential ray tracing features of Zemax® to realistically simulate different scenarios. Then we use MATLAB® to process the data obtained from Zemax® simulations.

We import the CAD files of all of the objects that we want to consider in our simulation, including sources (e.g., LEDs) and receivers (e.g., photodiodes), into Zemax® and properly position them to create our realistic 3D simulation environment. Then we define the light sources (like number, position and orientation of the sources) and characterize their specifications. We can either manually determine the light sources or import source files into Zemax®. In our case, we import and position source files which contain all the necessary information about the light sources such as spatial intensity distribution, SPD, and luminous flux (i.e., visible light output) of the LEDs. The unit of the light can be chosen as lumen, watt or joule.

Next, we insert proper detectors to function as receivers. There are various detector types in Zemax®; color, polar, rectangle, surface and volume detectors. Each of these detectors is used for a different detection purpose. For example, the polar detector is used to detect spatial intensity distribution of the light sources. We use rectangle detectors as the detecting surfaces of our receivers for detecting the power and path length information of received rays.

We, then, specify the optical properties of all the objects present in the simulation environment such as their reflection, refraction, transmittance, absorption and scattering properties. There are different ways to specify these properties. One way of doing so is to choose a material type for each object from the materials catalog of the Zemax®, if available, which already includes all the information about its optical properties. Another way is separately choosing these properties from coating and scattering catalogs that are available in the database of the Zemax®. One other way is manually defining these properties in Zemax®. For example, reflection, refraction, transmittance and absorption properties of the objects can be determined by defining the coating material properties of their surfaces. As another example, the type of reflection, such as specular, Lambertian or Gaussian, as discussed in [39], of each object or each surface/face of the objects can be decided by choosing a scattering model for the object of surface/face.

As the last operation in Zemax®, we set the simulation parameters and initiate the non-sequential ray tracing to obtain the power and path length data for each ray that is detected by the detectors. We then export these data for further calculations. Some of the main simulation parameters are the number of analysis rays (i.e., number of rays that will be traced for simulation) and considering polarization, splitting and/or scattering. Large numbers of analysis rays would provide more realistic results, but it will last longer to

trace all of the rays and complete the simulation. Similarly, including polarization, splitting and/or scattering properties of light while interacting with objects would also yield better results, but, again, with a cost of longer ray tracing time. The number of reflections of light rays to be taken into account in simulation can be determined, for example, by setting the value of minimum ray intensity or maximum intersections per ray. For detailed information about sources, detectors, optical specifications of materials, simulation parameters and more in Zemax® its help system [72] or its "Help PDF" file [73] can be used.

We import the data that we obtained from Zemax® simulations into MATLAB® and calculate CIR and other characteristics of the channel. The main steps that we use in ray tracing and CIR calculation for VLC are illustrated in Figure 10.

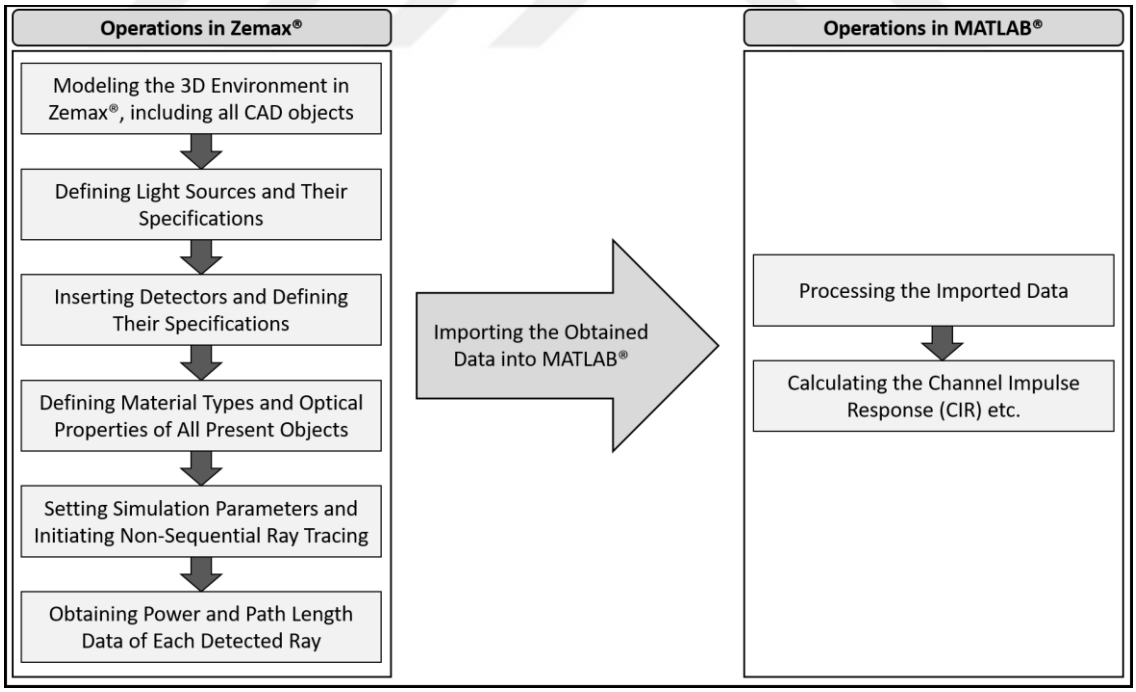

Figure 10: Main ray tracing and channel modeling steps for VLC

In this work, we assume the deployment of multiple ceiling luminaires where each LED luminaire consists of multi LED chips. Assume that there are N_L luminaires and each luminaire includes N_C LED chips.

Let $h_i(t), i = 1, \dots, N_C$, denote the individual optical CIR between the i^{th} LED chip and the receiver. It can be expressed as

$$h_i(t) = \sum_{j=1}^{N_r} P_{i,j}\, \delta(t - \tau_{i,j}) \tag{1}$$

where $P_{i,j}$ is the optical power of the j^{th} ray from the i^{th} LED chip, $\tau_{i,j}$ is the propagation time of the j^{th} ray from the i^{th} LED chip, $\delta(t)$ is the Dirac delta function and N_r is the number of rays received at the detector.

The optical CIR between the k^{th} luminaire, $k = 1, \dots, N_L$, and the receiver can be expressed as

$$h_k(t) = \sum_{i=1}^{N_C} h_i\left(t - \tau_{W_i}\right) \tag{2}$$

where τ_{W_i} is the wiring delay of the i^{th} LED chip and N_C is the number of LED chips inside the k^{th} luminaire. The overall optical CIR is then given as

$$h(t) = \sum_{k=1}^{N_L} h_k\left(t - \tau_{C_k}\right) = \sum_{k=1}^{N_L} \sum_{i=1}^{N_C} \sum_{j=1}^{N_r} P_{i,j}\, \delta\left(t - \tau_{i,j} - \tau_{W_i} - \tau_{C_k}\right) \tag{3}$$

where τ_{c_k} is the cabling delay of the k^{th} luminaire and N_L is the number of ceiling luminaires.

The frequency response of the optical channel can be further obtained through the Fourier transform, i.e.,

$$H(f) = F[h(t)] = \int_{-\infty}^{\infty} \sum_{k=1}^{N_L} \sum_{i=1}^{N_C} \sum_{j=1}^{N_r} P_{i,j}\, \delta\left(t - \tau_{i,j} - \tau_{W_i} - \tau_{C_k}\right) e^{-j2\pi t} dt\,. \quad (4)$$

Channel DC gain (H_0) is one of the most important features of a VLC channel, as it determines the achievable signal-to-noise ratio for a fixed transmitter power and is calculated as

$$H_0 = \int_0^{\infty} h(t)dt\,. \quad (5)$$

The path loss can, then, be expressed as

$$PL = -10\log_{10}[\int_0^{\infty} h(t)dt]\,. \quad (6)$$

The time dispersion parameters of channel, RMS delay spread and mean excess delay, are respectively given by

$$\tau_{RMS} = \sqrt{\frac{\int_0^{\infty}(t-\tau_0)^2\, h(t)\, dt}{\int_0^{\infty} h(t)dt}}, \quad (7)$$

$$\tau_0 = \frac{\int_0^{\infty} t \times h(t)dt}{\int_0^{\infty} h(t)dt}\,. \quad (8)$$

2.4 Numerical Results

In the simulation study, we consider a room with dimensions of 5 m × 5 m × 3 m as illustrated in Figure 11. Considering the layout in Figure 7, we assume four luminaires as $L_k, k = 1, \ldots, 4$, on the ceiling with equidistant spacing of 2 m. The LED luminaire has

a square shape with size of 0.6 m × 0.6 m and consists of 4 LED chips as $C_{k,i}, i = 1, \dots, 4$. Each LED chip radiates 5 W with a beam angle of 120^o. The receiver is designed in the form of a flat-top pyramid (see Figure 11) with four PDs, denoted as $D_l, l = 1, \dots, 4$, to provide a wide angle reception and to take advantage of the angular and spatial diversity [74, 75, 76]. The PDs are placed on the table at a height of 0.8 m. The field of view (FOV) semi-angle and area of the PD are 85^o and 1 cm^2, respectively. The cabling and wiring delay values are $\tau_{C_k} = 5\, ns/m$ [77] and $\tau_{W_i} = 6.5\, ns/m$ [78], respectively. The simulation parameters are summarized in Table 1.

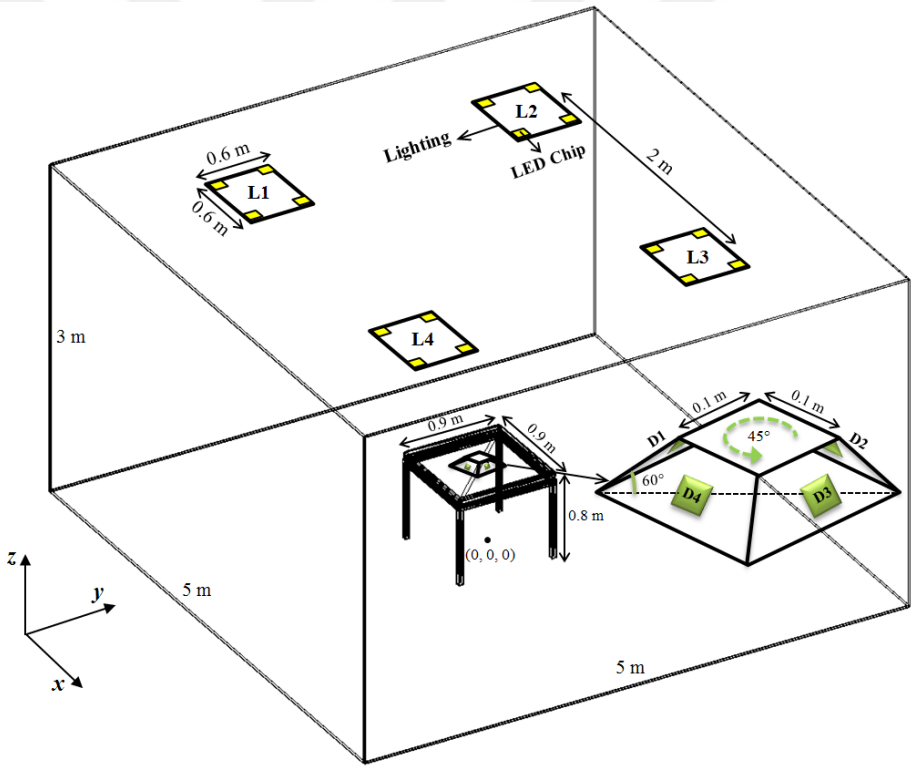

Figure 11: Indoor scenario under consideration

First, we consider cabling topologies 1 and 2 and ignore the wiring delays[1]. As a benchmark, we further consider the hypothetical case where the cables are delay-free.

[1] We ignore the effect of path loss related to data cables. In practice, an amplifier is used at VLC-enabled LED luminaire. Such an amplifier can be used to mitigate the effect of such losses.

Based on (3), the overall optical CIR $h(t)$ as seen by the PD D_1 is presented in Figure 12. It is observed from Figure 12 that in topology 1, we have one large peak and then one small. Since the cabling delays of four luminaires are the same, the signals from each luminaire are received at the same time. This results in one large peak followed by a small peak, the latter results from multipath reflections. In topology 2, it is observed that we have two large peaks followed by a small one. Two large peaks come from luminaire pairs (L_2 and L_3) and (L_1 and L_4) . It can also be noted that for the hypothetical case where the cables are delay-free, we have one large peak followed by a small one similar to topology 1. However, the large peak in this case occurs at 9 ns while the large peak in topology 1 occurs at 16 ns which is the result of cabling delay.

Table 1: Simulation parameters for scenario under consideration

Parameters	Values
Room Parameters	
Size of room (L × W × H)	5 m × 5 m × 3 m
Room	Wall: Plaster Floor: Pinewood Ceiling: Plaster
Furniture	Desk: Pinewood
Transmitter Parameters	
Size of luminaire	0.6 m × 0.6 m
Number of luminaires	4
Distance between luminaires	2 m
Number of LED chip per each luminaire	4
Power of each LED chip	5 W
Beam angle of LED chip (FWHM)	120^o
Cabling delay (τ_{C_k})	5 ns/m
Wiring delay (τ_{W_i})	6.5 ns/m
Receiver Parameters	
Number of PD	4
FOV of PD	85^o
Area of PD	1 cm^2
Distance between PDs	0.1 m

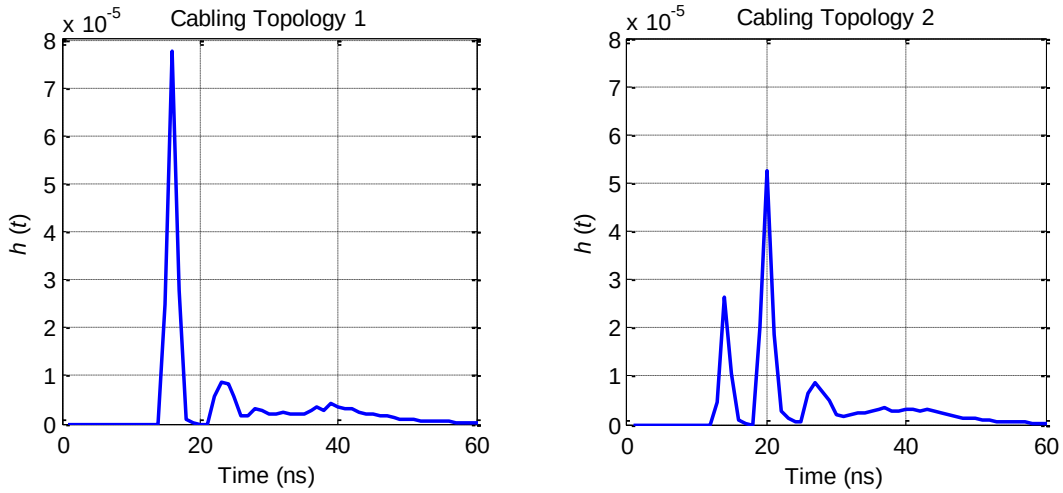

(a) (b)

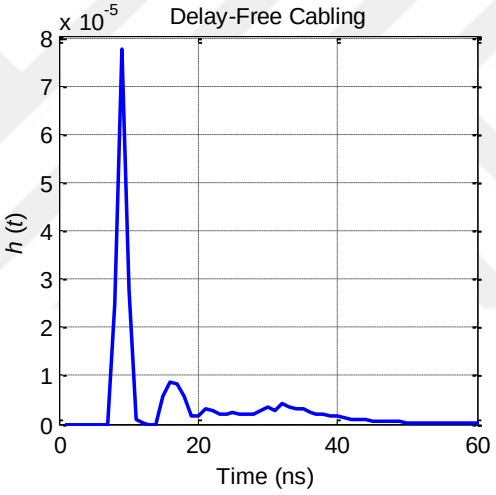

(c)

Figure 12: Overall optical CIRs (as received by the PD D_1) for (a) cabling topology 1, (b) cabling topology 2 and (c) delay-free cabling

Second, we consider wiring topologies 1, 2, 3 and 4 and ignore the cabling delays. As a benchmark, we further consider the hypothetical case where the wires are delay-free. Based on (2), the optical CIR $h_1(t)$ between luminaire L_1 and PD D_1 is presented in Figure 13. It is observed from Figure 13 that in wiring topologies 1 and 2, we have four large peaks followed by a small one. Four large peaks comes from LED chips $C_{1,1}$, $C_{1,2}$, $C_{1,3}$ and $C_{1,4}$ while the small one results from multipath reflections. In topology 3, it is

observed that we have one large peak and then one small. This is as a result of the fact that the wiring delays of four LED chips are the same. In topology 4, it is observed that we have two large peaks and then one small. Two large peaks comes from LED chip pairs ($C_{1,1}$ and $C_{1,2}$) and ($C_{1,3}$ and $C_{1,4}$). For the hypothetical delay-free case, we have one large peak and then one small similar to topology 3. It should be of course noted that the large peak in this case occurs at 9 ns, however, the large peak in topology 3 occurs at 13 ns which is the result of wiring delay.

Finally, we consider the effects of both wiring and cabling topologies in Figure 14. We assume the use of cabling topology 1 in conjunction with wiring topology 1 and 3. The hypothetical case of delay-free wiring and cabling is further included as a benchmark. It is observed from Figure 14.a that for cabling topology 1 in conjunction with wiring topology 1, we have four large peaks followed by a small one which is similar to CIR in Figure 13.a. It means that in this case the wiring topology is dominant for the channel characterization. Since the CIR in Figure 14.a is composed of the CIRs from four luminaires, its amplitude is larger than the CIR in Figure 13.a. Additionally, the first peak in the CIR in Figure 13.a (only wiring topology 1 is considered) occurs at 8 ns while the first peak of CIR in Figure 14.a (combined effect of wiring topology 1 and cabling topology 1 is considered) occurs at 15 ns as a result of cabling delay. It is further observed from the comparison of Figure 14.b and Figure 14.c that the CIR for the case of cabling topology 1 and wiring topology 3 has a similar behavior to the ideal case with only some delay. This is a result of the fact that these topologies have symmetrical structures, i.e., equal cabling and wiring lengths. In other words, all luminaires in cabling topology 1 and all LED chips in wiring topology 3 have identical cabling and wiring delays, respectively. Such a symmetrical wiring/cabling structure results in only an overall shift of the CIR.

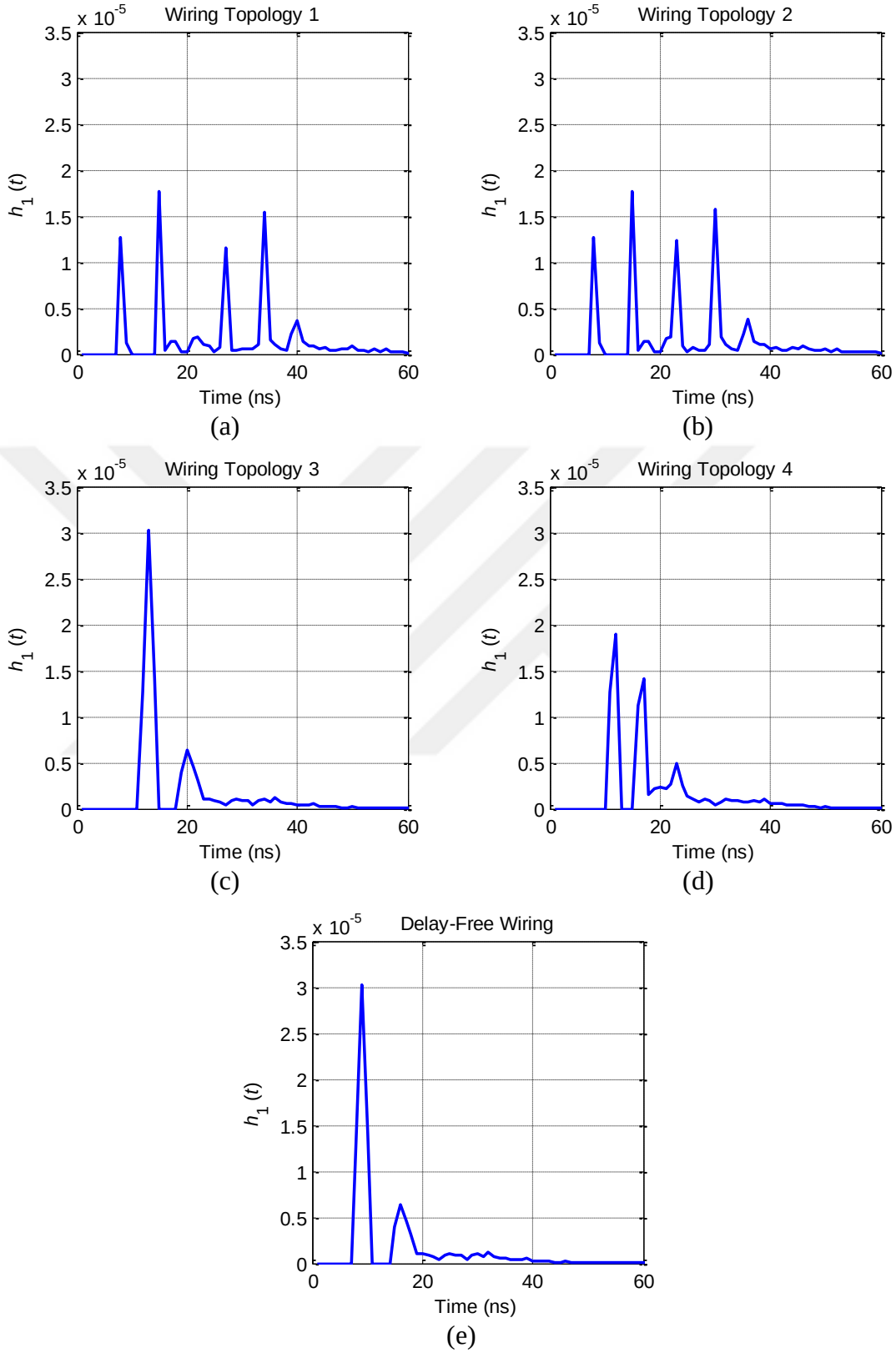

Figure 13: Optical CIRs from the luminaire (as received by the PD D_1) for (a) wiring topology 1, (b) wiring topology 2, (c) wiring topology 3, (d) wiring topology 4 and (e) delay-free wiring

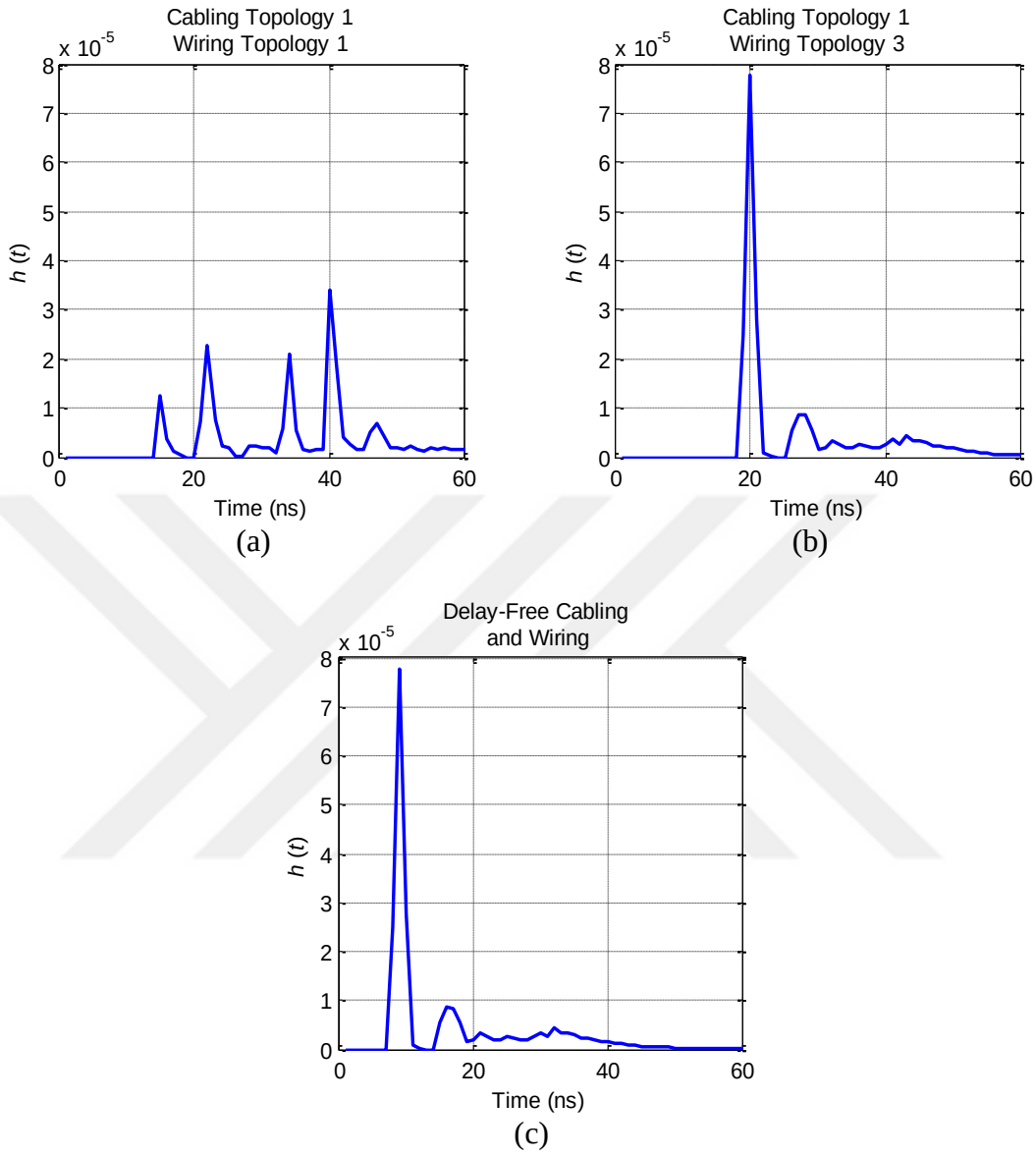

Figure 14: Overall optical CIRs (as received by the PD D_1) for (a) cabling topology 1 and wiring topology 1, (b) cabling topology 1 and wiring topology 3 and (c) delay-free cabling and wiring

The corresponding channel frequency responses of overall CIRs for these three cases are further illustrated in Figure 15. It is observed that frequency selectivity is introduced with respect to the ideal case of delay-free wiring and cabling. This will introduce limitations on the transmission bandwidth. According to the well-known 3dB-bandwidth definition [79], the bandwidth for the ideal case can be calculated as 12.74

MHz. This remains the same for the case where cabling topology 1 and wiring topology 3 are considered due to symmetrical structure. This reduces to 9.70 MHz for cabling topology 1 and wiring topology 1 where frequency selectivity is more pronounced.

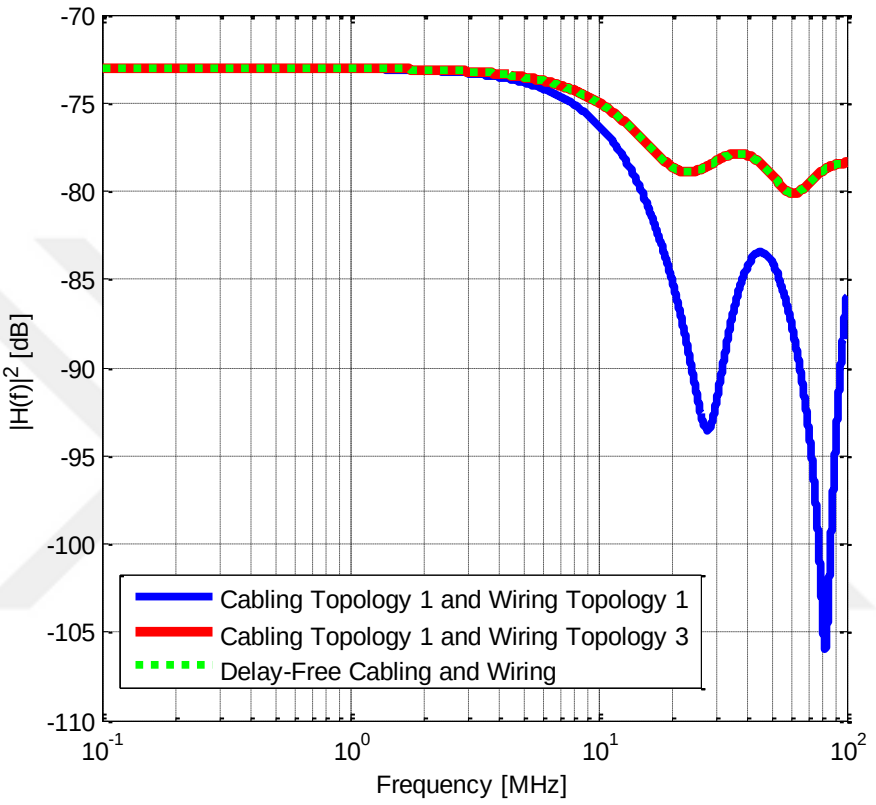

Figure 15: Channel frequency response of overall optical CIRs considering the combined effect of cabling and wiring delays

CHAPTER III

OUTDOOR LIGHTING DESIGN CONSIDERATIONS AND CHANNEL MODELING

3.1 Introduction

In this chapter, we discuss some main luminaire design parameters and analyze their effects on outdoor VLC. Then, we interpret and evaluate illumination requirements for outdoor VLC systems. We also consider a street lighting luminaire installation design scenario as a case study. Next, we present simulations for an I2P VLC channel modeling and obtain CIRs for a pedestrian moving between two street lighting luminaires. Then we use these CIRs to calculate channel DC gain, path loss, RMS delay spread and mean excess delay values.

3.2 Outdoor Lighting Design Considerations

LED luminaires are the source of light for illumination as well as the source of signal for VLC applications. Therefore, a better luminaire design would provide a better illumination and VLC performance. There are some luminaire design parameters that have direct influence on VLC systems. The parameters and effects discussed in section 2.2 for indoor lighting and indoor VLC also exactly apply for outdoor lighting and outdoor VLC. In addition, there are some other important LED luminaire components for outdoor VLC applications which are called as secondary optics.

3.2.1 Secondary Optics

Secondary optics, which refer to light guiding optical components, are of the main components of LED luminaires. They have different functions in a luminaire to achieve certain lighting requirements and might have significant effects on VLC channels as well. The efficiency of secondary optics is less important in indoor VLC, since the signal is attenuated less with less noise present in indoor environments. On the other hand, secondary optics become more significant for outdoor VLC applications for improving the optical signals which are attenuated more with more noise present in outdoor environments.

The most common secondary optics components that are used in LED luminaires are reflectors and lenses that are used to provide particular beam angles. The beam angle is defined as the full-width-at-half-max (FWHM) of the light intensity. Some luminaires, like down lights and panel lights, have wide beam angles to illuminate larger areas from closer distances, e.g., from ceilings. These luminaires commonly do not use reflectors or lenses. High bay lighting luminaires have narrow, medium or wide beam angles depending on the lighting application that they are used in. Projectors or flood lights, on the other hand, usually have narrow beam angles to illuminate particular areas from long distances like in stadium lighting and bridge lighting applications. They need reflectors or lenses that focus the wide beam angle of the light of LEDs into very narrow beam angles. There are also luminaires with asymmetrical beam angles. For example, street lighting luminaires have narrow vertical beam angles with wide horizontal beam angles (see Figure 20.a for an example). The vertical narrow beam is needed to focus the light to the road surfaces only and the horizontal wide beam is needed to distribute the light to

longer distances along the road. The beam angle is one of the most important parameters of luminaires. With a good lighting design optimization, the number of the luminaires that are used in a particular application can be reduced by changing the beam angle of the luminaires to meet certain illumination requirements. From communication point of view, reflectors and lenses define the power of the VLC signals in particular directions. Narrow beam angles would provide stronger signals in far distances, but with smaller coverage areas, while wide beam angles would provide signals with larger coverage areas for shorter distances. However, the use of reflectors or lenses in a luminaire would decrease the total light output of a luminaire and the power of the signals for VLC applications. Furthermore, lenses may have another disadvantage when a CSK modulation type with RGB LEDs is considered. Lenses provide particular beams for a luminaire by refracting the light of LEDs and they have wavelength dependent refractive indices. This would create some issues when a color shifting demodulation technique is considered, since the color shift could vary in different directions from the luminaire due to different refractions of different colors.

Another commonly used optical component in LED luminaires is the cover material which is a glass in most of the cases. In most LED luminaires a cover glass with a high optical transmittance is used for protection purposes. However, this glass decreases the total light output by a particular fraction, depending on its optical transmittance. A decrease in total light output implies a weaker optical signal power, when the luminaire is considered for VLC applications. Therefore, choosing a glass with higher optical transmittance would improve both illumination and communication performance of the luminaire. However, this, of course, would bring a small cost-up. It is also possible to avoid using a cover glass by using lenses with IP protections which would provide even

better illumination and communication performance. But, these kind of lenses are more expensive than normal ones. There are different glasses with different transmittances. The glass that is used in the tested luminaire has a transmittance of 90% (for normal incidence). Its transmittance can further be improved by applying an anti-reflecting coating. But this will bring some extra cost.

Paper-like reflector sheets are usually used in LED luminaires to enhance optical efficiency. They are highly reflective materials and are commonly used both in indoor and outdoor LED luminaires. Some of these reflectors are produced to have a sandy surface to provide diffuse reflections. A reflector sheet is placed on the PCB to reflect the light towards the illumination direction that comes backward directly from LEDs and the light reflected from lenses or from the cover glass and other parts of the luminaire. Using a reflector sheet would increase both total light output of a luminaire and the power of data signals for VLC applications.

To quantify the effects of secondary optics on illumination and VLC, we will evaluate the optical performance of paper-like reflector sheet, lenses and cover glass. The common disadvantage of these components is the reduction of optical efficiency of the luminaire and the power of the signal for VLC applications, except of the paper-like reflector sheets. We tested Vestel Ephesus M3S 90 street lighting luminaire, both with integrated sphere and goniophotometer in LED Optical Laboratory of Vestel to evaluate the effects of its secondary optics.

This luminaire has a luminous flux of 10400 lm with efficacy of 115 lm/W. Its secondary optics components are a paper-like reflector sheet which has a thickness of 188

microns, lenses with an asymmetrical beam angle (Figure 20.a) and a cover glass with 90% optical transmittance.

The luminaire was tested with different combinations of its secondary optics components to evaluate the overall optical efficiencies of the luminaire in each case and the effect of each component individually when used with other components. The test results of optical efficiencies of the luminaire with different combinations of optical components are shown in Table 2. The "X" symbols in Table 2 indicate which components were included during the test and an empty box/cell means the component was not included. The results shown in this table are the test results from both goniophotometer and integrating sphere.

In order to evaluate the optical effects of each component, we assume the efficiency of the luminaire without optical components to be 100% as a reference. As it is seen from test numbers 1, 2 and 3 in Table 2, while lenses and cover glass reduce the light output, the reflector sheet increases the optical efficiency of the luminaire. Table 3, Table 4 and Table 5 illustrate the individual effects of reflector sheet, lenses and cover glass, respectively, in different conditions which are derived from Table 2. The effect of reflector sheet changes from +1.61% up to +5.10% depending on use of different optical components, as shown in Table 3. Without other optical components, the reflector sheet has an effect of +3.01% on light output. However, when used with cover glass, its effect increases to +4.15%. This difference happens because the reflector sheet reflects only the light coming directly from LEDs when there is no cover glass, whereas it reflects both the light coming from LEDs and the light that is back-reflected by cover glass when the cover glass is used. On the other hand, the decrease in reflector sheet's effect to +1.61% when it is used with lenses is mainly caused by temperature increase around LEDs caused

by lenses. The effects of lenses and cover glass can similarly be evaluated from Table 4 and Table 5, respectively.

Table 2: Conditional efficiencies and net optical effects of optical components

Test	Ref. sheet	Lenses	Cover Glass	Efficiency	Net Effect
1				**100 % *(ref.)***	**0 %**
2	X			103.01 %	3.01 %
3		X		96.42 %	-3.58 %
4			X	90.22 %	-9.78 %
5	X	X		97.96 %	-2.04 %
6	X		X	93.32 %	-6.68 %
7		X	X	88.49 %	-11.51 %
8	X	X	X	93.00 %	-7.00 %

Table 3: Conditional net optical effects of reflector sheet

Component \ With	Lenses	Cover Glass	Net Effect
Reflector sheet	X	X	5.10 %
		X	4.15 %
	X		1.61 %
			3.01 %

Table 4: Conditional net optical effects of lenses

Component \ With	Ref. sheet	Cover Glass	Net Effect
Lenses	X	X	-0.34 %
		X	-1.24 %
	X		-4.90 %
			-3.58 %

Table 5: Conditional net optical effects of cover glass

Component \ With	Ref. sheet	Lenses	Net Effect
Cover Glass	X	X	-5.07 %
		X	-8.22 %
	X		-9.41 %
			-10.40 %

The total optical efficiency of the luminaire was tested to be 93% which provides an initial luminous flux of 10400 lm. This means that 7% of the light is lost due to using of secondary optics which is a luminous flux of 728 lm. Not using the reflector sheet

would cause an extra light loss of 4.51% which is a luminous flux of 469 lm, as seen from test numbers 7 and 8 of the Table 2. Similarly, the effect of other optical components can be evaluated from these tables which clearly show that secondary optics have significant effects on both illumination and VLC performance of a luminaire.

3.2.2 Illumination Requirements

The position and orientation of the luminaires have significant effects both on illumination performance and VLC channels. To illuminate a particular place with multiple luminaires, the position and orientation of each luminaire is determined and optimized to meet the lighting requirements for that place like average illuminance (lux) values and uniformity which would also affect the VLC channel. For instance, street lighting luminaires can be considered as an example which will be discussed in details in this section, where we will discuss the placement and orientation of street lighting luminaires and possible effects on both illumination and VLC channels.

Street lighting design has high significance for a comfortable and safe journey. Due to this significance, standards, which define lighting requirements for street lighting applications, are developed and are being revised with developing technology. One of these standards is European standard EN 13201 (EN 13201-1, EN13201-2, EN 13201-3, EN 13201-4 and EN 13201-5) [80] which provides detailed explanations for street lighting requirements. There are three lighting classes depending on lighting situations; M for motorized traffic areas, C for conflict areas, and P for pedestrian and low speed areas. Each of these classes are also divided into six sub-classes depending on speed limit, traffic volume, traffic composition, separation of carriageway, junction density, existence of parked vehicles, ambient luminosity etc.. To meet all lighting requirements, firstly, the

road lighting class should be determined and then, for a given street lighting luminaire, the pole parameters should be optimized.

As a case study, we present a street lighting luminaire installation that meets the lighting requirements, as defined by the standard, and discuss some implications of these requirements on VLC systems. We consider using a street lighting luminaire and design the luminaire installation using DIALux®, a free professional lighting design software [81]. DIALux® calculates pole assembly parameters, such as pole separation and height, for all possible arrangements within user defined constraints and limits for the considered luminaire to meet all lighting class requirements based on a chosen standard (e.g., EN 13201) which is available in DIALux® database. It also simulates a chosen arrangement and provides a detailed report of lighting parameters.

Table 6: Lighting requirements for M3 lighting class

Class	Luminance of the road surface of the carriageway for the dry road surface condition			Disability glare	Lighting of surroundings
	Dry condition			Dry condition	
	L_{av} in cd/m^2 [minimum maintained]	U_0 [minimum]	U_l [minimum]	TI % [maximum]	SR [minimum]
M3	1.00	0.40	0.60	15	0.50

We consider a road lighting class of M3, as described by EN 13201-1. The lighting requirements for M3 class according to EN 13201-2 are summarized in Table 6. The parameters in Table 6 are as follows. L_{av} is the average road surface illuminance, U_0 is the overall uniformity of the illuminance, U_l is the longitudinal uniformity of the luminance, TI is the threshold increment, and SR is the surround ratio. These parameters are calculated and measured according to EN 13201-3 and EN 13201-4. The street profile under consideration is outlined in Table 7.

Table 7: Street profile under consideration

Roadway	Width: 10.50 m
Number of Lanes	2
Surface Properties	Tarmac: R3, q0: 0.070
Light Loss Factor (LLF)	0.89
Lighting Class	M3

We also consider Vestel Ephesus M3S 90 street lighting luminaire for simulations. DIALux® made the calculations for pole assembly parameters and listed possible arrangements out of which we chose the arrangement with pole assembly parameters listed in Table 8. The parameters in Table 8 are illustrated in Figure 16.

Table 8: Optimized pole parameters

Selected Luminaire	Vestel Ephesus M3S 90
Arrangement	Double Row, Opposing
Luminaires per Pole	1
Pole Distance	25.00 m
Mounting Height (1)	7.00 m
Height	6.90 m
Overhang (2)	-0.50 m
Boom Angle (3)	0^o
Boom Length (4)	1.00 m

With above configuration we made the simulations in DIALux® and the results are presented as follows. 3D and false color renderings are shown in Figure 17. Illuminance (E_v) isolines are illustrated in Figure 18 with calculated illuminance parameters listed in Table 9. The calculation field results are illustrated in Table 10.

The below DIALux® simulations show that the pole parameters, i.e., positions and orientations of street lighting luminaires have significant effects on both illumination and VLC performances. Figure 17.b and Figure 18 show the illuminance values on different points, consequently the VLC signal powers in different positions from the luminaires which would be different for different pole parameters. Similar to this case,

the positions and orientations of any type of luminaire would have significant effects both from illumination and communication points of view.

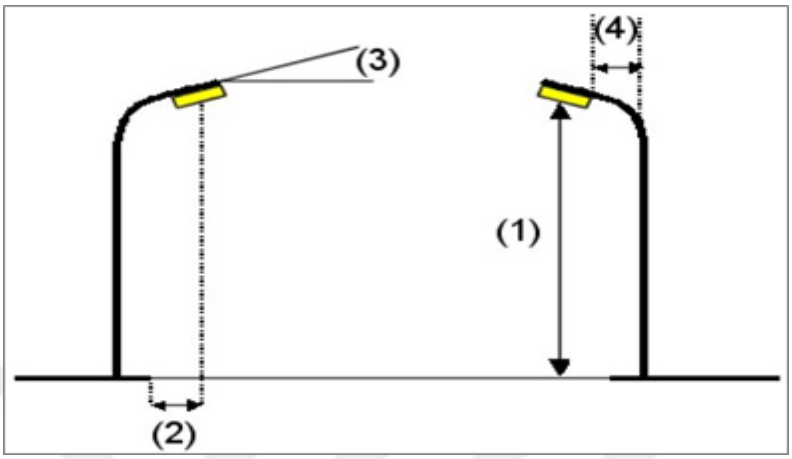

Figure 16: Pole parameters

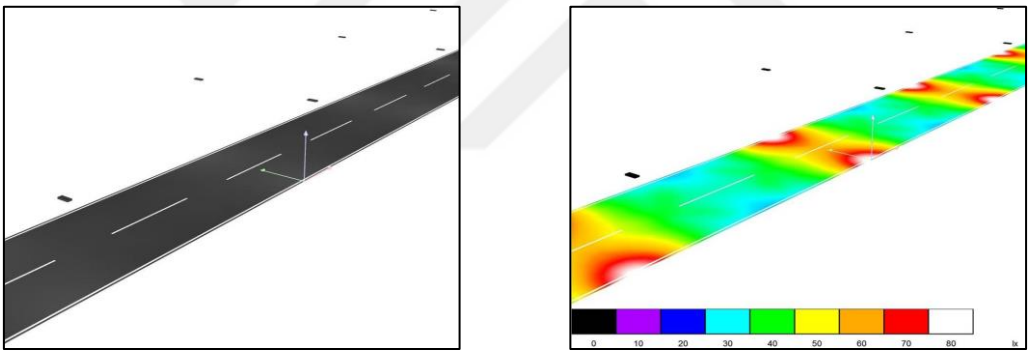

(a) (b)

Figure 17: (a) 3D view and (b) false color rendering of the street scenario

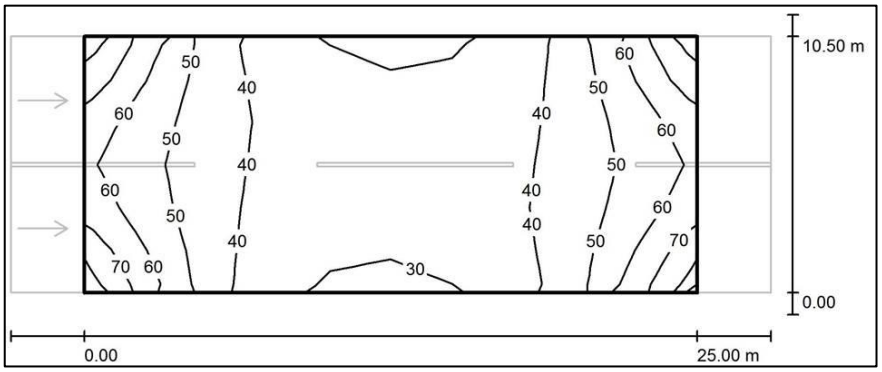

Figure 18: Illuminance (E_v) isolines

Table 9: Calculated illuminance parameters

E_{av} [lx]	E_{min} [lx]	E_{max} [lx]	u0	E_{min} / E_{max}
44	29	74	0.659	0.392

Table 10: Calculated field values and requirements

	L_{av} [cd/m^2]	U_0	U_l	TI [%]	SR
Calculated values	2.64	0.69	0.73	8	0.55
Required values according to class	≥ 1.00	≥ 0.40	≥ 0.70	≤ 15	≥ 0.50
Fulfilled/Not fulfilled (OK/NOK)	OK	OK	OK	OK	OK

3.3 Outdoor VLC Channel Modeling

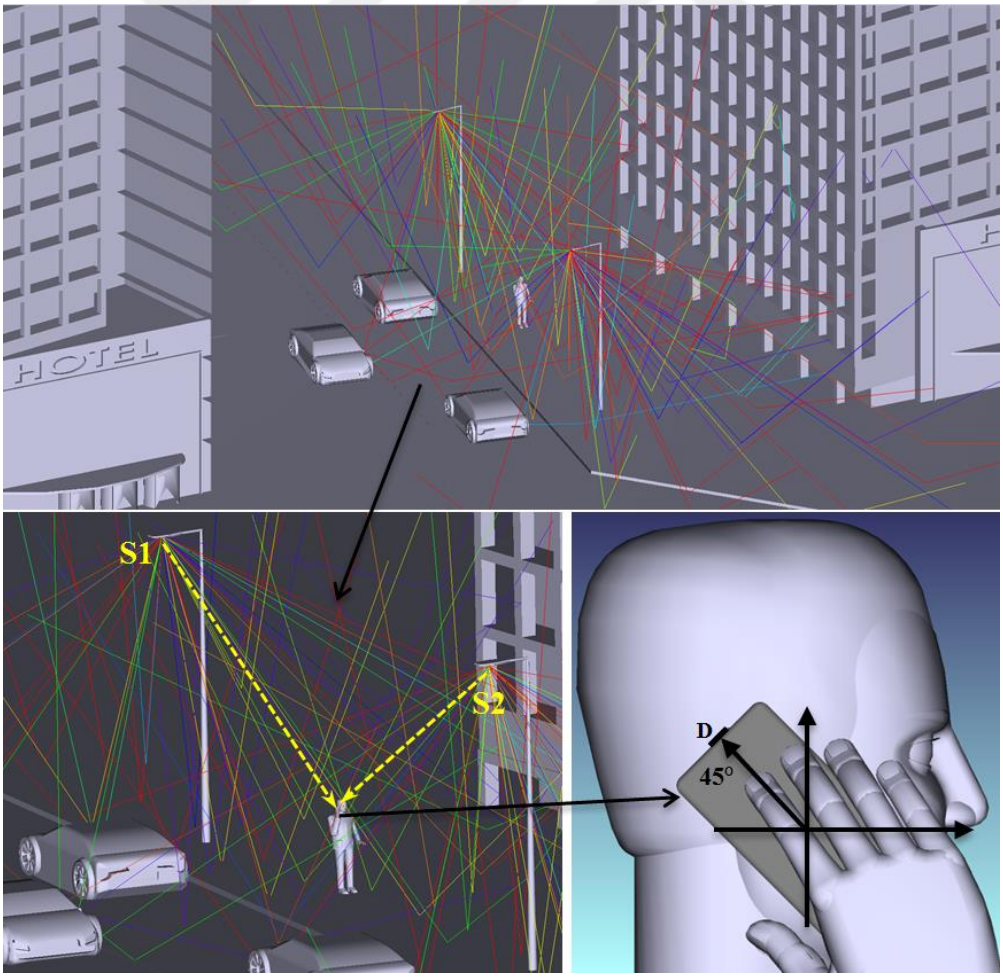

Figure 19: Outdoor scenario under consideration

We consider a VLC usage scenario (i.e., metropolitan-main road) shown in Figure 19. This scenario is composed of vehicles, buildings, roads/fields, street lights and pedestrian. We assume that coating materials of buildings, cars and street lamp poles are respectively concrete, black gloss paint and galvanized steel metal. The road type is assumed as tarmac – R3 with the coating material of asphalt.

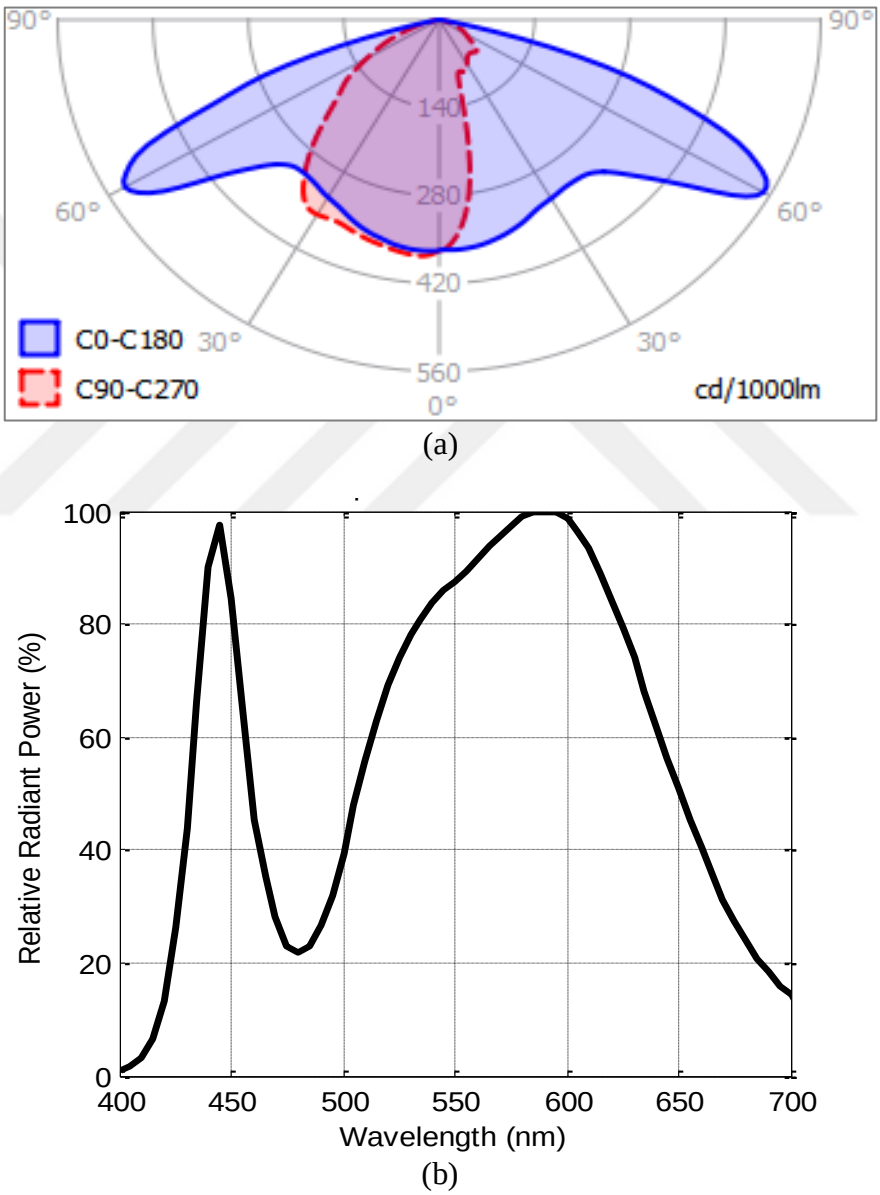

Figure 20: (a) Relative intensity distribution in polar diagram and (b) relative spectral power distribution of Vestel Ephesus M3S 90

We assume only two Ephesus M3S 90 luminaires, Vestel brand street lighting luminaires, with spacing of 14 m. Spatial intensity distribution and relative SPD of luminaire are presented in Figure 20. The important parameters of this street lighting luminaire are listed in Table 11.

Table 11: Product specifications of Vestel Ephesus M3S-90

Electrical input power	90 W
Luminous flux	10400 lm
Efficacy	115 lm/W
Color temperature (CCT)	4000K
CRI	≥ 70
Beam angle	Asymmetric

We consider a pedestrian who has internet access through street lights (see Figure 19). Pedestrian body is modeled as CAD object with different coating materials for different parts of the body. Specifically, its head and hands are modeled as absorbing objects while cotton clothes and black gloss shoes are assumed. Non-sequential ray tracing features of Zemax® are used to calculate the detected power and path lengths from source to detector for each ray. These are used to obtain the CIR between the light sources and the detector. The detector can be placed at any point where the CIR is desired to be computed. The ray tracing and channel modeling steps are discussed in section 2.3.1 and briefly shown in Figure 10. Here, we assume that the pedestrian walks on the trajectory between two street lights. We assume that he/she holds a cell phone in hand next to his/her ear and the detector is located on the phone. The orientation of human body (where he/she is facing) changes according to the direction of the way while the rotation and location of cell phone (i.e., 45^o rotation and at a height of 1.8 m) in his/her hand are fixed with respect to his/her ear. The FOV and the area of the detector are 85^o and 1 cm^2, respectively. The simulation parameters are listed in Table 12.

Table 12: Simulation parameters

Street light specifications	**Vestel Ephesus M3S 90** 0.5 W per each luminaire
Receiver specifications	**Area:** 1 cm^2 **Field of view (FOV):** 85^o
Road specifications	**Material:** Asphalt **Tarmac:** R3
Specifications of objects and surfaces	**Buildings:** Concrete **Street lamp poles:** Galvanized steel metal **Cars:** Black gloss paint
Pedestrian (user)	**Shoes:** Black gloss paint **Head & hands:** Absorbing **Clothes:** Cotton **Cell phone:** Black gloss paint

Based on the approach summarized above and given scenario, we obtain CIRs for all points with 1 m inter-distance along that trajectory for a maximum span of 14 m (i.e., denoted as P1, …, P14). Let $h_k(t)$ denote the individual optical CIR between the i^{th} street light and the receiver. $h(t) = \sum_{k=1}^{2} h_k(t)$ represents the combined optical CIR from two street lights. Once we obtain CIRs, we can calculate several channel parameters such as channel DC gain, path loss, RMS delay spread and mean excess delay.

Based on the given scenario and the simulation parameters (see Table 12), we present the CIRs between the pedestrian and the street lights in Figure 21.

Table 13 summarizes the channel parameters for the configuration under consideration. The CIRs presented in Figure 21 show that the communication is only LOS in this scenario with negligible multipath reflections (seen as small dots in the figures) reaching the receiver.

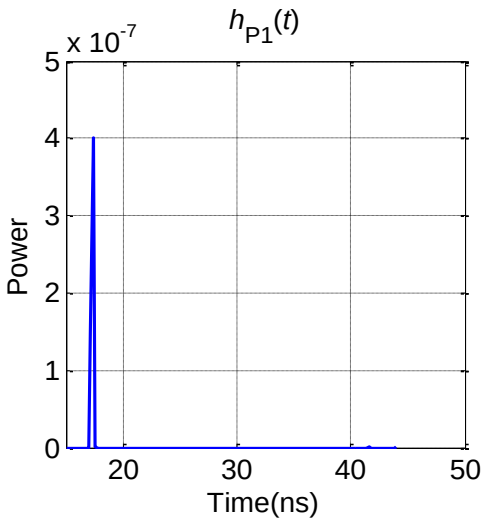
$h_{P1}(t)$
x 10^-7
Power
Time(ns)

(a)

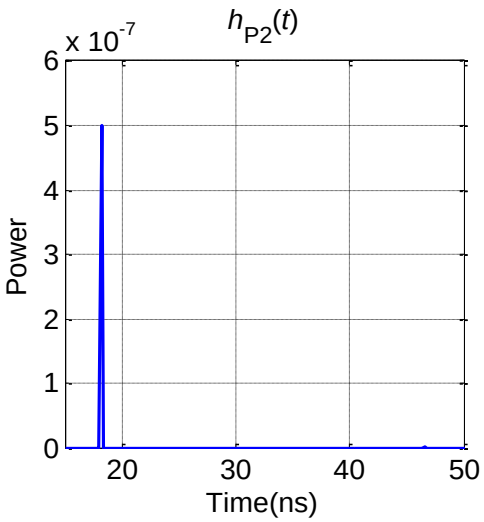
$h_{P2}(t)$
x 10^-7
Power
Time(ns)

(b)

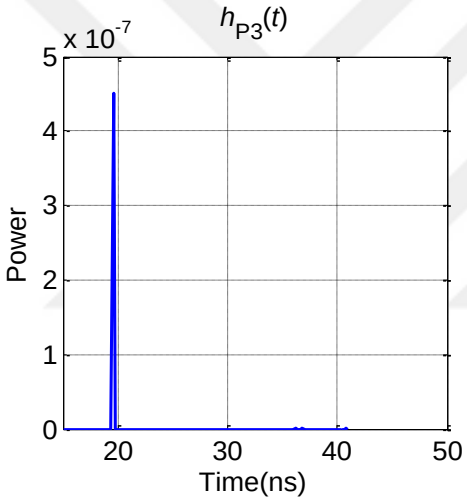
$h_{P3}(t)$
x 10^-7
Power
Time(ns)

(c)

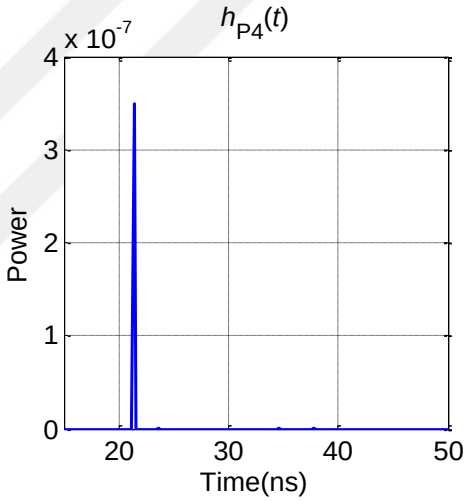
$h_{P4}(t)$
x 10^-7
Power
Time(ns)

(d)

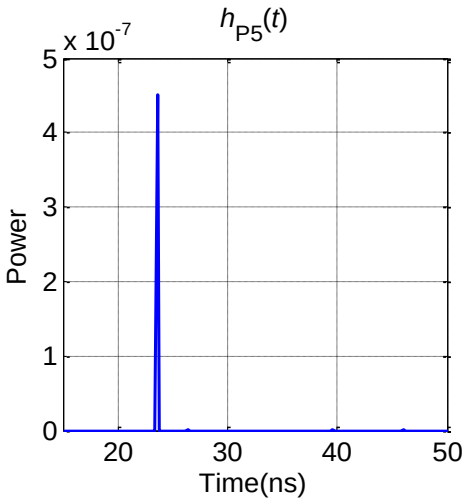
$h_{P5}(t)$
x 10^-7
Power
Time(ns)

(e)

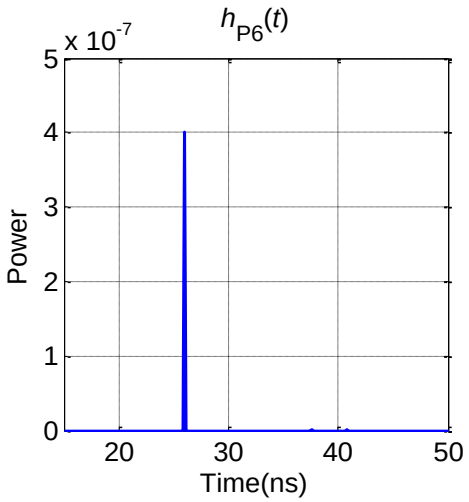
$h_{P6}(t)$
x 10^-7
Power
Time(ns)

(f)

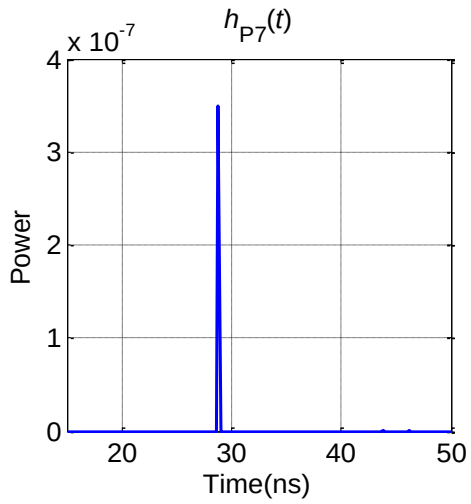
$h_{P7}(t)$
x 10^-7
Power
Time(ns)

(g)

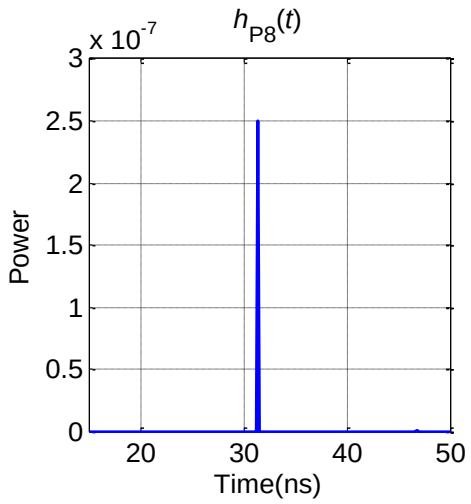
$h_{P8}(t)$
x 10^-7
Power
Time(ns)

(h)

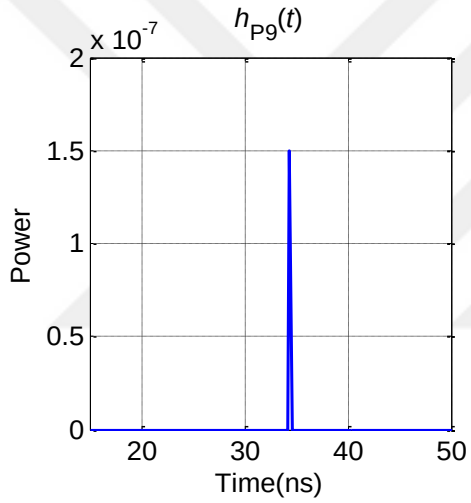
$h_{P9}(t)$
x 10^-7
Power
Time(ns)

(i)

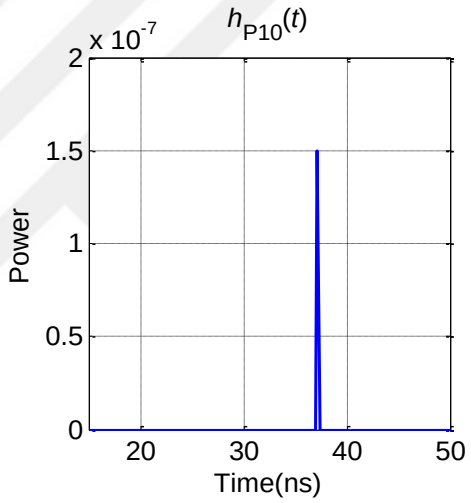
$h_{P10}(t)$
x 10^-7
Power
Time(ns)

(j)

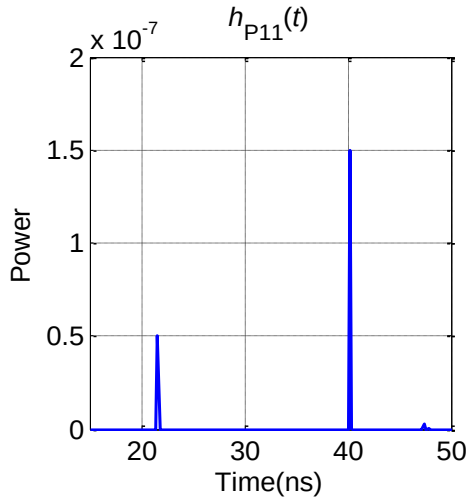
$h_{P11}(t)$
x 10^-7
Power
Time(ns)

(k)

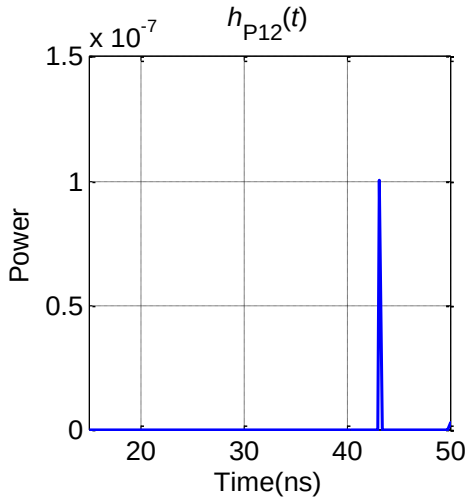
$h_{P12}(t)$
x 10^-7
Power
Time(ns)

(l)

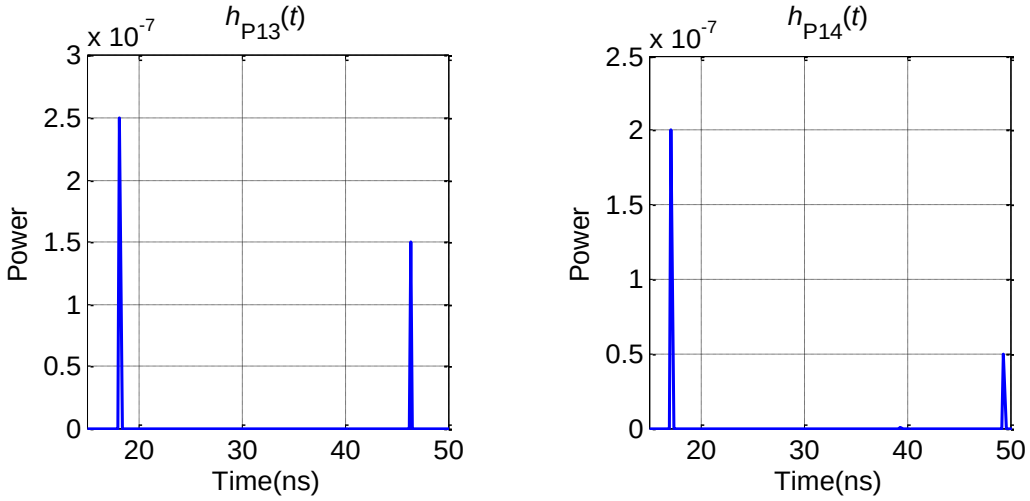

Figure 21: (a) – (n) CIRs for scenario under consideration

Table 13: Channel parameters for scenario under consideration

	τ_0 (ns)	τ_{RMS} (ns)	H_0	PL (dB)
P1	18.01	0.52	5.50×10^{-7}	62.59
P2	19.01	0.83	5.00×10^{-7}	63.01
P3	20.01	0.55	4.50×10^{-7}	63.46
P4	22.06	1.70	3.50×10^{-7}	64.55
P5	24.03	1.24	4.50×10^{-7}	63.46
P6	26.02	0.89	4.00×10^{-7}	63.97
P7	29.03	0.92	3.50×10^{-7}	64.55
P8	32.02	0.86	2.50×10^{-7}	66.02
P9	35.01	0.67	1.50×10^{-7}	68.23
P10	38.03	1.05	1.50×10^{-7}	68.23
P11	36.48	8.57	2.03×10^{-7}	66.92
P12	44.17	2.21	1.02×10^{-7}	69.91
P13	29.57	13.66	4.00×10^{-7}	63.97
P14	24.41	12.84	2.50×10^{-7}	66.02

CHAPTER IV

CONCLUSIONS

In this thesis, we adopted a realistic channel modeling approach based on non-sequential ray tracing features of Zemax® for indoor and outdoor VLC scenarios. Instead of using ideal Lambertian sources that are typically used in existing works, we used realistic photometric files of commercial LEDs and LED luminaires to simulate the scenarios in Zemax®.

In Chapter II, we discussed how some indoor lighting design considerations could affect the performance of a VLC system followed by channel modeling of an indoor scenario. Then we discussed typical electro-optical characteristics of LEDs which play an important role in designing the wiring topologies of LED luminaires and choosing or designing PSUs (i.e., LED drivers). We also provided detailed and industry-standard explanations of typical cabling and wiring topologies for LED luminaires and chose various cabling and wiring topologies to be considered in our indoor VLC scenario. Then, we adopted a realistic channel modeling approach [39] for channel modeling of the indoor scenario and obtained CIRs using non-sequential ray tracing with higher order number of reflections. We, then, presented numerical results. Our results show that cabling and wiring topologies introduce delays with significant effects. Therefore, symmetrical cabling and wiring topologies, i.e., topologies with equal cabling and wiring lengths, are more favorable. Furthermore, frequency selectivity is more pronounced for asymmetrical topologies.

In Chapter III, we provided an extensive analysis of some main outdoor lighting design considerations and their effects on the performance of VLC. We demonstrated and experimentally quantified how main secondary optics of an LED luminaire, namely lenses, reflectors, cover glasses and paper-like reflector sheets affect the performance of both lighting and VLC. Furthermore, we discussed how the number, positions and orientations of luminaires are significant for both lighting and VLC applications. We showed that a well optimized luminaire installation can reduce the number of luminaires that are used to illuminate a particular area with a better VLC performance and, hence, reduce the cost. As a case study, we provided a detailed example of street lighting design that met the illumination requirements according to European standard EN 13201 (EN 13201-1, EN13201-2, EN 13201-3, EN 13201-4 and EN 13201-5) [80] and considered the impacts of these standard requirements on VLC systems.

We deployed the realistic channel modeling approach in [39] using Zemax® for 3D modeling of the environment and simulations for an outdoor I2P VLC scenario. Simulations were carried out in Zemax® for the pedestrian at 14 different equidistant points between two street lighting luminaires. The simulation results were then imported into MATLAB® and processed to obtain the CIRs. We also calculated channel DC gain, path loss, RMS delay spread and mean excess delay values using these CRIs.

When the indoor and outdoor VLC scenarios are compared, we see that the indoor VLC has combinations of both LOS and non-LOS signals on the receiver side. On the other hand, we notice that our outdoor VLC scenario seems to have only LOS signals received with negligibly low non-LOS signals.

BIBLIOGRAPHY

[1] Cisco White Paper, "Cisco visual networking index: Global mobile data traffic forecast update, 2016-2017," Feb. 2017.

[2] S. Riurean, R. Stoica and M. Leba, "Visible Light Communication for Audio Signals," *International Journal of Communications,* vol. 2, pp. 24-27, 2017.

[3] P. Rost, C. J. Bernardos, A. D. Domenico, M. D. Girolamo, M. Lalam, A. Maeder, D. Sabella and D. Wübben, "Cloud technologies for flexible 5G radio access networks," *IEEE Commun. Mag.,* vol. 52, no. 5, pp. 68-76, 2014.

[4] Huawei White Paper, "Global connectivity index," 2016.

[5] US Federal Communications Comission White Paper, "Connecting America: the national broadband plan".

[6] R. Gummadi, D. Wetherall, B. Greenstein and S. Seshan, "Understanding and mitigating the impact of RF interference on 802.11 networks," *SIGCOMM Comput. Commun. Rev.,* vol. 37, no. 4, pp. 385-396, 2007.

[7] A. Akella, G. Judd, S. Seshan and P. Steenkiste, "Self-management in chaotic wireless deployments," in *Proceedings of the 11th Annual International Conference on Mobile Computing and Networking (MobiCom '05)*, Cologne, 2005.

[8] G. N. Gibson, "Constructive and Destructive Interference," University of Connecticut, [Online]. Available: http://www.phys.uconn.edu/~gibson/Notes/Section5_2/Sec5_2.htm. [Accessed 15 January 2019].

[9] C. W. Commander, P. M. Pardalos, V. Ryabchenko, S. Uryasev and G. Zrazhevsky, "The wireless network jamming problem," *J. Comb. Optim.,* vol. 14, no. 4, pp. 481-498, 2007.

[10] S.-H. Ye, Y.-S. Kim, H.-S. Lyou, M.-S. Kim and J. Lyou, "Verification of electromagnetic effects from wireless devices in operating nuclear power plants," *Nuclear Eng. and Technol.,* vol. 47, no. 6, pp. 729-737, 2015.

[11] P. D. Ewing, M. K. Howlader and J. Dion, "Wireless network security in nuclear facilities," in *NPIC&HMIT 2010*, Las Vegas, 2010.

[12] M. K. Howlader, P. D. Ewing and J. Dion, "Issues associated with deploying wireless systems in nuclear facilities," in *NPIC&HMIT 2010*, Las Vegas, 2010.

[13] H. Ma, "Coordinated transmission for visible light communication systems," Ph.D. Dissertation, Univ. of British Columbia, Vancouver, 2017.

[14] M. Agiwal, A. Roy and N. Saxena, "Next generation 5G wireless networks: a comprehensive survey," *IEEE Commun. Surveys & Tut.,* vol. 18, no. 3, pp. 1617-1655, 2016.

[15] L. U. Khan, "Visible light communication: Applications, architecture, standardization and research challenges," *Digital Communications and Networks,* vol. 3, no. 2, pp. 78-88, 2017.

[16] H. Elgala, "A Study on the Impact of Nonlinear Characteristics of LEDs on Optical OFDM," Ph.D. dissertation, SES School of Eng. and Science, Jacobs Univ., Bremen, 2010.

[17] A. G. Bell, "Selenium and the Photophone," *Nature,* vol. 22, no. 569, pp. 500-503, 1880.

[18] E. O. Dieterich, "Influence of annealing on the characteristics of light-sensitive selenium," MS Thesis, State University of Iowa, 1914.

[19] M. Uysal, C. Capsoni, Z. Ghassemlooy, A. Boucouvalas and E. Udvary, Optical wireless communications: an emerging technology, Switzerland: Springer International Publishing, 2016.

[20] S. Dimitrov and H. Haas, Principles of LED light communications: towards networked Li-Fi, Cambridge, United Kingdom: Cambridge University Press, 2015.

[21] N. Sklavos, M. Hübner, D. Goehringer and . P. Kitsos, "VLC Technology for Indoor LTE Planning," in *System-level design methodologies for telecommunication*, Switzerland, Springer, Cham, 2014, p. 28.

[22] T. Komine and M. Nakagawa, "Fundamental analysis for visible-light communication system using LED lights," *IEEE Transactions on Consumer Electronics,* vol. 50, no. 1, pp. 100-107, 2004.

[23] S. Sagar, D. Lal and S. Dahiya, "Visible light communication," *International Journal of Engineering Research and Development,* vol. 11, no. 1, pp. 36-40, 2015.

[24] S. M. Riurean, A. A. Nagy, M. Leba and A. C. Ionica, "A small step in VLC systems – a big step in Li-Fi implementation," *IOP Conference Series: Materials Science and Engineering,* vol. 294, no. 1, p. 012047, 2018.

[25] "Li-Fi Technology Applications - Hospital, Office, Home, etc.," Oledcomm, [Online]. Available: https://www.oledcomm.com/solutions/. [Accessed 16 January 2019].

[26] M. Wright, "Philips Lighting deploys LED-based indoor positioning in Carrefour hypermarket," LEDs Magazine, 21 May 2015. [Online]. Available: https://www.ledsmagazine.com/articles/2015/05/philips-lighting-deploys-led-based-indoor-positioning-in-carrefour-hypermarket.html. [Accessed 16 January 2019].

[27] A. Jovicic, *Qualcomm ® Lumicast TM : A high accuracy indoor positioning system based on visible light communication April 2016,* Qualcomm, 2016.

[28] Press Release, *GE Intelligent Lighting to Transform Retail Experience through Qualcomm Collaboration,* General Electric (GE), 2015.

[29] Press Release, *Qualcomm and Acuity Brands collaborate to commercially deploy Qualcomm Lumicast Technology for precise indoor location services in more than 100 retail locations,* Qualcomm, 2016.

[30] "LuxLive 2017 Review," DMN, 27 November 2017. [Online]. Available: https://dmndesignbuild.com/luxlive-exhibition-2017-review/. [Accessed 16 January 2019].

[31] "World's first Li-Fi light panel launched," Lux Magazine, 14 February 2018. [Online]. Available: https://luxreview.com/article/2018/02/world-s-first-li-fi-light-panel-launched/. [Accessed 16 January 2019].

[32] D. Flynn, "Airbus wants to upgrade WiFi to the speed of light," Australian Business Traveller, 10 June 2016. [Online]. Available: https://www.ausbt.com.au/airbus-wants-to-upgrade-wifi-to-the-speed-of-light. [Accessed 16 January 2019].

[33] j. J. George, M. H. Mustafa, N. M. Osman, N. H. Ahmed and D. M. Hamed, "A survey on visible light communication," *International Journal of Engineering And Computer Science,* vol. 3, no. 2, pp. 3805-3808, 2014.

[34] P. H. Pathak, X. Feng, P. Hu and P. Mohapatra, "Visible light communication, networking, and sensing: A survey, potential and challenges," *IEEE Commun. Surveys Tuts.,* vol. 17, no. 4, pp. 2047-2077, 2015.

[35] M. Uysal, F. Miramirkhani, O. Narmanlioglu, T. Baykas and E. Panayirci, "IEEE 802.15.7rl reference channel models for visible light communications," *IEEE Commun. Mag.,* vol. 55, no. 1, pp. 212-217, 2017.

[36] A. Behlouli, P. Combeau and L. Aveneau, "MCMC methods for realistic indoor wireless optical channels simulation," *J. Lightwave Technol.,* vol. 35, no. 9, pp. 1575-1587, 2017.

[37] J. Ding, I. Chih-Lin and Z. Xu, "Indoor optical wireless channel characteristics with distinct source radiation patterns," *IEEE Photon. J.,* vol. 8, no. 1, pp. 1-15, 2016.

[38] H. Schulze, "Frequency-domain simulation of the indoor wireless optical communication channel," *IEEE Trans. Commun.,* vol. 64, no. 6, pp. 2551-2562, 2016.

[39] F. Miramirkhani and M. Uysal, "Channel modeling and characterization for visible light communications," *IEEE Photon. J.,* vol. 7, no. 6, pp. 1-16, 2015.

[40] K. Lee, H. Park and J. R. Barry, "Indoor channel characteristics for visible light communications," *IEEE Commun. Lett.,* vol. 15, no. 2, pp. 217-2019, 2011.

[41] F. Miramirkhani, O. Narmanlioglu, M. Uysal and E. Panayirci, "A mobile channel model for VLC and application to adaptive system design," *IEEE Commun. Lett.,* vol. 21, no. 5, pp. 1035-1038, 2017.

[42] P. Chvojka, S. Zvanovec, P. A. Haigh and Z. Ghassemlooy, "Channel characteristics of visible light communications within dynamic indoor environment," *J. Lightwave Technol.,* vol. 33, no. 9, pp. 1719-1725, 2015.

[43] Y. Xiang, M. Zhang, M. Kavehrad, M. I. S. Chowdhury, M. Liu, J. Wu and X. Tang, "Human shadowing effect on indoor visible light communications channel characteristics," *Opt. Eng.,* vol. 53, no. 8, pp. 086113-086113, 2014.

[44] G. Ren, S. He and Y. Yang, "An improved recursive channel model for indoor visible light communication systems," *Inf. Technol. J.,* vol. 12, no. 6, pp. 1245-1250, 2013.

[45] A. R. Ndjiongue and H. C. Ferreira, "An overview of outdoor visible light communications," *Transactions on Emerging Telecommunications Technologies,* vol. 29, no. 7, p. e3448, 2018.

[46] F. Miramirkhani, "Channel modeling and characterization for visible light communications: indoor, vehicular and underwater channels," PhD dissertation, Graduate School of Sciences and Engineering, Ozyegin University, Istanbul, Turkey, 2018.

[47] A. Arora, "Exploring non-sequential mode in OpticStudio," Zemax, 8 October 2014. [Online]. Available: https://customers.zemax.com/os/resources/learn/knowledgebase/exploring-non-sequential-mode-in-zemax. [Accessed 30 January 2019].

[48] "Zemax OpticStudio optical design software illumination design," https://www.zemax.com/products/opticstudio/.

[49] S. Safaraliev, F. Miramirkhani and M. Uysal, "Effect of LED wiring and cabling topologies on visible light communication channels," in *2017 10th International Conference on Electrical and Electronics Engineering (ELECO)*, Bursa, Turkey, 2017.

[50] O. Narmanlioglu, R. C. Kizilirmak, F. Miramirkhani, S. Safaraliev, S. M. Sait and M. Uysal, "Effect of wiring and cabling topologies on the performance of distributed MIMO OFDM VLC systems," *IEEE Access,* vol. 7, pp. 52743-52754, 25 April 2019.

[51] M. Saadi, L. Wattisuttikulkij, Y. Zhao and P. Sangwongngam, "Visible light communication: opportunities, challenges and channel models," *International Journal of Electronics & Informatics,* vol. 2, no. 1, pp. 1-11, 2013.

[52] D. C. O'Brien, L. Zeng, H. Le-Minh, G. Faulkner, J. W. Walewski and S. Randel, "Visible light communications: Challenges and possibilities," in *2008 IEEE 19th International Symposium on Personal, Indoor and Mobile Radio Communications*, Cannes, 2008.

[53] M. Noshad and M. Brandt-Pearce, "Can Visible Light Communications Provide Gb/s Service?," *arXiv:1308.3217,* 2013.

[54] J. Grubor, S. C. J. Lee, K.-D. Langer, T. Koonen and J. W. Walewski, "Wireless High-Speed Data Transmission with Phosphorescent White-Light LEDs," in *33rd European Conference and Exhibition of Optical Communication - Post-Deadline Papers (published 2008)*, Berlin, 2007.

[55] H. L. Minh, D. O'Brien, G. Faulkner, L. Zeng, K. Lee, D. Jung and Y. Oh, "High-Speed Visible Light Communications Using Multiple-Resonant Equalization," *IEEE Photon. Technol. Lett.,* vol. 20, no. 14, pp. 1243-1245, 2008.

[56] H. L. Minh, D. O'Brien, G. Faulkner, L. Zeng, K. Lee, D. Jung, Y. Oh and E. T. Won, "100-Mb/s NRZ Visible Light Communications Using a Postequalized White LED," *IEEE Photon. Technol. Lett.,* vol. 21, no. 15, pp. 1063-1065, 2009.

[57] A. M. Khalid, G. Cossu, R. Corsini, P. Choudhury and E. Ciaramella, "1-Gb/s Transmission Over a Phosphorescent White LED by Using Rate-Adaptive Discrete Multitone Modulation," *IEEE Photonics Journal,* vol. 4, no. 5, pp. 1465-1473, 2012.

[58] S.-W. Wang, F. Chen, L. Liang, S. He, Y. Wang, X. Chen and W. Lu, "A high-performance blue filter for a white-led-based visible light communication system," *IEEE Wireless Communications,* vol. 22, no. 2, pp. 61-67, 2015.

[59] V. Wood and V. Bulović, "Colloidal quantum dot light-emitting devices," *Nano Rev.,* vol. 1, no. 1, p. 5202, 2010.

[60] S. J. Cho, D. Maysinger, M. Jain, R. Beate, S. Hackbarth and F. M. Winnik, "Long-term exposure to CdTe quantum dots causes functional impairments in live cells," *Langmuir,* vol. 23, no. 4, pp. 1974-1980, 2007.

[61] I. Dursun, C. Shen, M. R. Parida, J. Pan, S. P. Sarmah, D. Priante, N. Alyami, J. Liu, M. I. Saidaminov, M. S. Alias, A. L. Abdelhady, T. K. Ng, O. F. Mohammed, B. S. Ooi and O. M.

Bakr, "Perovskite Nanocrystals as a Color Converter for Visible Light Communication," *ACS Photonics,* vol. 3, no. 7, pp. 1150-1156, 2016.

[62] CIE, Commission internationale de l'Eclairage proceedings, 1931, Cambridge: Cambridge University Press, 1932.

[63] T. Smith and J. Guild, "The C.I.E. colorimetric standards and their use," *Trans. Opt. Soc.,* vol. 33, no. 3, p. 73, 1931.

[64] Technical Report, "Health effects of artificial light," *Scientific Committee on Emerging and Newly Identified Health Risks (SCENIHR),* pp. 1-118, 2012.

[65] A. Bradford, "How blue LEDs affect sleep," LIVE SCIENCE, 26 February 2016. [Online]. Available: https://www.livescience.com/53874-blue-light-sleep.html. [Accessed 21 January 2019].

[66] L. J. Kraus, "Human and Environmental Effects of Light Emitting Diode (LED) Community Lighting," AMERICAN MEDICAL ASSOCIATION, 2016. [Online]. Available: http://darkskyarkansas.com/wp-content/uploads/2017/01/DarkSideBlueLight.pdf. [Accessed 21 January 2019].

[67] M. Kayaba, K. Iwayama, H. Ogata, K. Kiyono, M. Satoh and K. Tokuyama, "The effect of nocturnal blue light exposure from light-emitting diodes on wakefulness and energy metabolism the following morning," *Environ. Health Prev. Med.,* vol. 19, no. 5, pp. 354-361, 2014.

[68] M. Wright, "Seoul Semiconductor and Toshiba Materials introduce broad-spectrum LED technology (UPDATED)," LEDs Magazine, 26 June 2017. [Online]. Available: https://www.ledsmagazine.com/articles/2017/06/seoul-semiconductor-and-toshiba-materials-introduce-broad-spectrum-led-technology.html. [Accessed 21 January 2019].

[69] "SunLike," Seoul Semiconductor, [Online]. Available: http://www.seoulsemicon.com/en/technology/Sunlike/. [Accessed 21 January 2019].

[70] Press Release, "Seoul Semiconductor's SunLike series natural spectrum LEDs adopted by JingDong for new LED desk lamps in China," Seoul Semiconductor, 03 January 2019. [Online]. Available: http://www.seoulsemicon.com/en/company/press/press-release/. [Accessed 21 January 2019].

[71] "LM281B+," Samsung, [Online]. Available: https://www.samsung.com/led/lighting/mid-power-leds/2835-leds/lm281b-plus/. [Accessed 24 November 2018].

[72] A. Yates, "How to Use the Help System with OpticStudio," Zemax, 19 March 2014. [Online]. Available:

https://customers.zemax.com/os/resources/learn/knowledgebase/how-to-use-the-in-line-help-files-with-opticstudio. [Accessed 30 January 2019].

[73] "Getting started with OpticStudio 15," May 2015. [Online]. Available: https://customers.zemax.com/ZMXLLC/media/PDFLibrary/Brochures/OpticStudio_GettingStarted.pdf?ext=.pdf. [Accessed 30 January 2019].

[74] P. F. Mmbaga, J. Thompson and H. Haas, "Performance analysis of indoor diffuse VLC MIMO channels using angular diversity detectors," *Journal of Lightwave Technology,* vol. 34, no. 4, pp. 1254-1266, 2016.

[75] A. Burton, Z. Ghassemlooy, S. Rajbhandari and S.-K. Liaw, "Design and analysis of an angular-segmented full-mobility visible light communications receiver," *Transactions on Emerging Telecommunications Technologies,* vol. 25, no. 6, pp. 591-599, 2014.

[76] A. Nuwanpriya, S.-W. Ho and C. S. Chen, "Indoor MIMO visible light communications: Novel angle diversity receivers for mobile users," *IEEE Journal on selected areas in communications,* vol. 33, no. 9, pp. 1780-1792, 2015.

[77] M. Uysal and R. C. Kizilirmak, "Single color networks: OFDM-based visible light broadcasting," in *2015 International Conference on Computer, Communications, and Control Technology (I4CT)*, Kuching, 2015.

[78] H. Zumbahlen, "Printed circuit board (PCB) design issues," in *Basic linear design, ch. 12*, Analog Devices, 2007.

[79] A. F. Molisch, Wireless Communications, John Wiley & Sons, 2012.

[80] "EN 13201 Standards for Road lighting all parts," European Standards, [Online]. Available: https://www.en-standard.eu/csn-en-13201-1-4-road-lighting/.

[81] "DIALux," https://www.dial.de/en/dialux/.

VITA

Sadi Safaraliev received the B.Sc. degree in Physics from Middle East Technical University, Ankara, Turkey, in 2014, where he mainly concentrated on Optics and Optoelectronics. He enrolled as a graduate student in Electrical and Electronics Engineering Department at Ozyegin University in January 2016, Istanbul, Turkey, working toward his M.Sc. degree under supervision of Prof. Murat Uysal. He received his M.Sc. degree in Electrical and Electronics Engineering in June 2019. His academic research interests include optics, optoelectronics, VLC and channel modeling.

Sadi is currently a Senior Optical Design Engineer at Vestel Electronics Corp., Manisa, Turkey, since October 2014, where he is mainly responsible for optical design, tests and verification of lighting products, including designing of optical components (e.g., reflectors and lenses), benchmarking, and researching new products. His main professional fields of interest are LED lighting, automotive lighting, imaging and non-imaging optics, holographic displays and VLC.